FINAL TECHNICAL REPORT

15 November 1982 - 14 November 1984

"Influence of Scattering on Q in the Lithosphere"

By

Anton M. Dainty, Robert M. Duckworth, and An Tie

School of Geophysical Sciences
Georgia Institute of Technology
Atlanta, Georgia 30332

Principal Investigator: Anton M. Dainty (404) 894-2860

Contract Amount: $85,000

Contract Termination Date: 14 November 1984

Program Manager: William J. Best (202) 767-4908

Sponsored by:

Advanced Research Projects Agency (DOD)
ARPA Order No. 4397, Am. No. 3
Monitored by NP under Grant No. AFOSR-83-0037
Program Code: 3D60

UNCLASSIFIED

SECURITY CLASSIFICATION OF THIS PAGE

REPORT DOCUMENTATION PAGE

1a. REPORT SECURITY CLASSIFICATION UNCLASSIFIED	1b. RESTRICTIVE MARKINGS
2a. SECURITY CLASSIFICATION AUTHORITY	3. DISTRIBUTION/AVAILABILITY OF REPORT Approved for public release; distribution unlimited.
2b. DECLASSIFICATION/DOWNGRADING SCHEDULE	
4. PERFORMING ORGANIZATION REPORT NUMBER(S)	5. MONITORING ORGANIZATION REPORT NUMBER(S) AFOSR-TR- 85-0101
6a. NAME OF PERFORMING ORGANIZATION Georgia Tech Research Institute; 6b. OFFICE SYMBOL (If applicable)	7a. NAME OF MONITORING ORGANIZATION Air Force Office of Scientific Research
6c. ADDRESS (City, State and ZIP Code) Atlanta, GA 30332	7b. ADDRESS (City, State and ZIP Code) Bolling Air Force Base Washington, DC 20332
8a. NAME OF FUNDING/SPONSORING ORGANIZATION Defense Advanced Research Projects Agency; 8b. OFFICE SYMBOL (If applicable)	9. PROCUREMENT INSTRUMENT IDENTIFICATION NUMBER AFOSR-83-0037
8c. ADDRESS (City, State and ZIP Code) 1400 Wilson Blvd. Arlington, VA 27709	10. SOURCE OF FUNDING NOS. PROGRAM ELEMENT NO. 61102F; PROJECT NO. 2309; TASK NO. A1; WORK UNIT NO.
11. TITLE (Include Security Classification) ~~Investigation~~ Influence of Scattering and Q in the Lithosphere	
12. PERSONAL AUTHOR(S) Anton M. Dainty, Robert M. Duckworth, and An Tie	
13a. TYPE OF REPORT Final Technical; 13b. TIME COVERED FROM 11/15/82 TO 11/14/84	14. DATE OF REPORT (Yr., Mo., Day); 15. PAGE COUNT
16. SUPPLEMENTARY NOTATION	
17. COSATI CODES: FIELD; GROUP; SUB. GR.	18. SUBJECT TERMS (Continue on reverse if necessary and identify by block number)

19. ABSTRACT (Continue on reverse if necessary and identify by block number)

This project examined the contribution of scattering to the attenuation of short pulses within the crust. Coda decay and excitation for local events were examined at Mammoth Lakes and Morgan Hill, California; Monticello, South Carolina; and New Brunswick, Canada, in the frequency range 3-50 Hz. For short times (less than 10 seconds), the total turbidity determined from coda decay was about 0.1 km^{-1} for all regions, applying a magnitude bias of 0.2 in m_b if 10 km of such material is traversed. Since the total turbidity is independent of frequency, implying geometrical scattering, this would not be detectable by spectral ratio methods. The backscattering turbidity determined from coda excitation at short times indicates strong scattering in the upper crust, especially for frequencies

(Continued on reverse)

20. DISTRIBUTION/AVAILABILITY OF ABSTRACT UNCLASSIFIED/UNLIMITED ☒ SAME AS RPT. ☐ DTIC USERS ☐	21. ABSTRACT SECURITY CLASSIFICATION UNCLASSIFIED
22a. NAME OF RESPONSIBLE INDIVIDUAL Tato Dir Kadoski	22b. TELEPHONE NUMBER (Include Area Code) (202) 767-4906; 22c. OFFICE SYMBOL NP

DD FORM 1473, 83 APR EDITION OF 1 JAN 73 IS OBSOLETE.

UNCLASSIFIED

SECURITY CLASSIFICATION OF THIS PAGE

19. ABSTRACT (Continued)

in the 3-10 Hz range. At times longer than 10-15 seconds for the codas from the eastern North American regions, Monticello and New Brunswick, the coda energy appeared to be channeled into a horizontally propagating mode such as Lg. The total turbidity for this portion of the coda was lower than for the short codas, about 0.01 km^{-1}, indicating less scattering, a result born out by the backscattering turbidity. Codas from California, however, did not show this phenomenon, indicating either that this mode is not present or that it is more strongly scattered. This result indicates that attenuation for Lg can be estimated from the coda after 10 seconds, as proposed by other workers. All of the scattering observed in this study occurs in the crust; since in situations where single scattering occurs the backscattering turbidity is about 1% of the total turbidity, velocity fluctuations may be responsible. Multiple scattering occurred in the short codas at frequencies around 3 Hz.

TABLE OF CONTENTS

TECHNICAL REPORT SUMMARY

This project examined the contribution of scattering to the attenuation of short pulses within the crust. Coda decay and excitation for local events were examined at Mammoth Lakes and Morgan Hill, ~~California,~~ Monticello, ~~South Carolina,~~ and New Brunswick, Canada, in the frequency range 3-50 Hz. For short times (less than 10 seconds), the total turbidity determined from coda decay was about 0.1/km^{-1} for all regions, applying a magnitude bias of 0.2 in m_b if 10 km of such material is traversed. Since the total turbidity is independent of frequency, implying geometrical scattering, this would not be detectable by spectral ratio methods. The backscattering turbidity determined from coda excitation at short times indicates strong scattering in the upper crust, especially for frequencies in the 3-10 Hz range. At times longer than 10-15 seconds for the codas from the eastern North American regions, Monticello and New Brunswick, the coda energy appeared to be channeled into a horizontally propagating mode such as Lg. The total turbidity for this portion of the coda was lower than for the short codas, about 0.01/km^{-1}, indicating less scattering, a result born out by the backscattering turbidity. Codas from California, however, did not show this phenomenon, indicating either that this mode is not present or that it is more strongly scattered. This result indicates that attenuation for Lg can be estimated from the coda after 10 seconds, as proposed by other workers. All of the scattering observed in this study occurs in the crust; since in situations where single scattering occurs the

backscattering turbidity is about 1% of the total turbidity, velocity fluctuations may be responsible. Multiple scattering occurred in the short codas at frequencies around 3 Hz.

INFLUENCE OF SCATTERING ON Q IN THE LITHOSPHERE

By

Anton M. Dainty, Robert M. Duckworth, and An Tie

Introduction

If accurate assessments are to be made of the size and nature of a seismic event (explosion or earthquake), we must have a good understanding of the changes in amplitude and waveform of seismic waves as they travel from the source to a more or less distant receiver. Conventionally, this problem has been divided into two parts: "geometrical spreading" and "attenuation". These terms derive from a combination of theoretical considerations of idealised problems (ray theory in homogeneous, isotropic--at least piecewise--media) and some simple experimental observations showing that in real media a certain amount of seismic energy is apparently lost, perhaps to heat, compared to ray theory calculations. Anything that can be fitted into the theory of wave propagation in ideal, elastic media is usually called "geometrical spreading", while anything that can be described as loss of energy from the seismic wavefield is usually called "attenuation". In the simplest cases, the effect of geometrical spreading on amplitude often has the form of a frequency independent power law (e.g., I/R for spherical spreading), whereas the effect of attenuation on amplitude is described by a frequency dependent exponential law ($\exp[-\pi fR/QV]$, where Q is the quality factor and V is the wave velocity).

The real media encountered in the earth differ from ideal homogeneous elastic media in several ways. One is the phenomenon of conversion of the elastic energy of the seismic wavefield to heat mentioned above. Another is the presence of inhomogeneity of the elastic parameters and the density, probably on all linear scales. Some of the effects of the large scale inhomogeneity can be included in geometrical spreading explicitly--for example, the depth dependent inhomogeneity commonly observed in the earth. However, much of the inhomogeneity is too complex to be handled by deterministic methods and has to be considered as producing random scattering, whose effects can only be calculated as a statistical average. In considering these effects, a difficulty emerges. Whilst conceptually the effect of scattering is geometrical spreading, since energy does not leave the total seismic wavefield, operationally the effect of scattering may in part be like that of attenuation. For example, if a pulse confined in time propagates through a scattering medium, seismic energy will be scattered out of the time frame containing the pulse. If amplitude measurements are made only in the time frame containing the pulse, a common procedure, the amplitude will appear to have attenuated with an exponential law as $\exp[-GR/2]$, where G is a parameter known as the total turbidity, or the total scattering cross-section per unit volume.

In the work reported on here, we have endeavored to find the attenuation effect due to scattering in the lithosphere of the earth at high frequencies (above 1 Hz) in the sense described above. Since sources of particular interest (explosions) and receivers are located near the surface of the earth, all seismic waves encounter this environment; for regional phases this is the only environment encountered. Scattering has been assessed by examination of the coda of local earthquakes.

Since the coda consists of backscattered energy, we have separately assessed the backscattering turbidity (or backscattering cross-section per unit volume) determined from the size of the coda relative to the direct S wave and the total quality factor Q, expressed as an apparent total turbidity, determined from the coda decay rate. We have done this for two regions of California--Mammoth Lakes and Morgan Hill--and two regions in eastern North America--Monticello, South Carolina, and New Brunswick, Canada.

Theoretical Summary

In this section we will discuss, in order, the characterisation of scatterers and scattering, attenuation of a short pulse due to scattering, and the theory of local coda. Part of this material is covered in earlier reports submitted under this grant and included as Appendices 1 and 2--references will be made to the Appendices as appropriate.

The simplest case of scattering occurs when there is only one scatterer of prescribed shape. Whilst the case of scattering in an elastic medium has recently been treated by Wu and Aki (1984), many useful ideas about scattering can be illustrated by simpler acoustic cases. Let us consider a sound wave in a uniform acoustic medium of amplitude A_I and frequency f incident on a body of different acoustic properties located at the origin of spherical polar coordinate R, θ, ϕ. At large distances from the body the amplitude of the scattered sound wave A_s will be given by (Clay and Medwin, 1977):

$$A_s^2 = A_I^2 \cdot \sigma(\theta,\phi,f) \cdot (1/R^2) \tag{1}$$

This indicates that far away from the scattering body the body appears as a point source of magnitude $A_I \sqrt{\sigma(\theta,\phi,f)}$, with an angular dependence of radiation controlled by the quantity $\sigma(\theta,\phi,f)$ known as the differential cross-section. An important special case is $\theta = \pi$ (backscattering in the strict sense), then $\sigma = \sigma_b(f)$, the backscattering cross-section. Figure 1 shows σ_b for a rigid, fixed sphere in an acoustic medium. An important feature of Figure 1 is the division of scattering into two types. At low frequencies, the backscattering cross section increases strongly (as f^4) with frequency (Rayleigh scattering) as long as the radius of the sphere is appreciably less than the wavelength. Geometrical scattering occurs at higher frequencies when the wavelength is shorter than the radius of the sphere. Under these conditions, the backscattering cross-section for geometrical scatter is larger than for Rayleigh scatter, but independent of frequency. Also, for both cases, the backscattering cross-section is proportional to the physical cross-section. These results taken together indicate that if a variety of scatterers of different sizes are insonified by a sound wave of a given wavelength, the larger scatterers that are in the geometrical scattering regime will dominate, other things being equal.

If there are N scatterers per unit volume, the differential cross-section per unit volume, or differential turbidity, is

$$g(\theta,\phi,f) = N\sigma(\theta,\phi,f) \tag{2}$$

The energy scattered in direction θ,ϕ from a small volume ΔV is the

$$A_s^2 = A_I^2\, g(\theta,\phi,f) \cdot \Delta V/R^2 \tag{3}$$

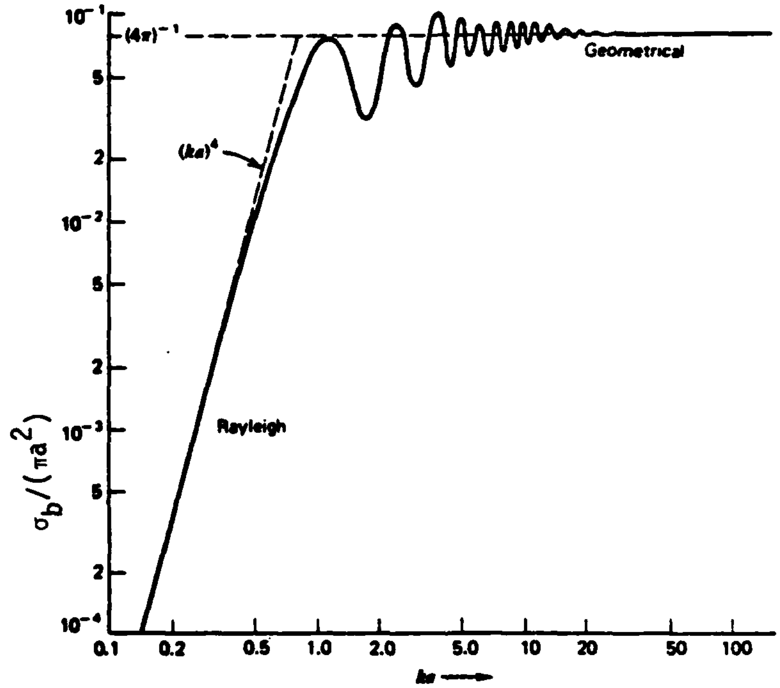

Figure 1. Backscattering Function For a Rigid, Fixed, Sphere of Radius a. Derived from Stenzel (1938), (Clay and Medwin, 1977).

This formulation leads to a second method of describing scatterers, in terms of a random medium. Chernov (1960), using results from earlier workers, showed that if an acoustic medium contained velocity or density fluctuations ("scatterers"), only a knowledge of the autocorrelation of these fluctuations is necessary to calculate $g(\theta,\phi,f)$.

To apply (3) to the attenuation of a short pulse, note that scattered energy may be effectively lost from the pulse. In the discussion that follows, the pulse will be discussed in terms of its Fourier components. Energy deflected at small angles to the original direction of travel (forward scatter) will not be lost, however; Sato (1982) suggests that most energy scattered at angles of 30° or less is included in the original pulse, causing fluctuations of amplitude and phase. The total loss of intensity from a wave encountering a volume ΔV of scatterers can be found by enclosing the volume in a sphere of radius R and integrating the scattered intensity given by (3) over the surface of the sphere, excluding energy scattered at angle θ less than $\theta_c \sim 30°$, as discussed above. Here $\theta = 0$ is taken as the direction of propagation of the incident wave. Then the intensity loss

$$\begin{aligned} \Delta I_I = \Delta(A_I^2) &= -A_I^2 \cdot \Delta V \cdot \int_0^{2\pi} d\phi \int_{\theta_c}^{\pi} d\theta \cdot \sin\theta \cdot g(\theta,\phi,f) \\ &= -I_I \cdot \Delta V \cdot G(f) \qquad (4) \end{aligned}$$

In (4) the I's represent intensity and G(f) is known as the total turbidity. Using (2), we may also define

$$\sigma_t(f) = \int_0^{2\pi} \int_{\theta_c}^{\pi} d\theta \cdot \sin\theta \cdot \sigma(\theta,\phi,f) \ , \qquad (5)$$

the total scattering cross-section.

If ΔV in (4) is taken as a slab consisting of a unit area face in the plane of the wavefront and a side Δx perpendicular to the wavefront

$$\Delta I_I = -G(f) \cdot I_I \cdot \Delta x \tag{6}$$

If we consider the wave to propagate through a scattering medium that may be split up into such slabs, (6) can be integrated (Wu, 1982) to obtain

$$I_I = I_0 \exp[-G(f)x] \tag{7}$$

This may be expressed formally in terms of a scattering Q, Q_s, if Q_s is defined by

$$I_I = I_0 \exp[-2\pi fx/(Q_s C)] \tag{8}$$

where C is the sound velocity. Then

$$1/Q_s = G(f)C/(2\pi f) \tag{9}$$

If the medium also attenuates anelastically, parameterised by an intrinsic Q, Q_I, then the total Q will be given by (Dainty, 1981)

$$1/Q = 1/Q_I + 1/Q_s \tag{10}$$

$$= 1/Q_I + G(f)C/(2\pi f) \tag{11}$$

The frequency dependence expected for Q_s may be deduced from the results presented earlier for a rigid, immovable sphere. For low frequencies Rayleigh scattering occurs; generally, G(f) has a similar frequency dependence as $g(\pi,f)$, that is to say, G(f) increases with frequency as f^4 leading to $Q_s \alpha 1/f^3$. For high frequencies, the wavelength will be short and geometrical scattering may occur. Then G(f) will be independent of frequency and $Q_s \alpha f$. Dainty (1981) has examined two cases of shear wave Q in which this may be true for frequencies above 1 Hz in the lithosphere. Dainty (1984) and Wu (1982) discuss the frequency dependence expected for Q_s when the scattering medium is characterised as a random medium rather than by discrete scatterers. Dainty (1984; included as Appendix 2 of this report) demonstrated that if there is a length scale associated with the random medium, and discontinuities within the medium, then at high frequencies (wavelength shorter than the length scale) the frequency dependence of $g(\theta,\phi,f)$ and G(f) will be the same as that for geometrical scattering, i.e., independent of frequency.

The theory presented so far is for the acoustic case. Wu and Aki (1984) have presented results for the elastic case. They find that, in addition to P to P and S to S scattering, which are analogous to acoustic scattering, there is also P to S and S to P scattering ("mode conversion"). However, there are no backscattered mode conversions (i.e., scattered back directly along the ray path). P to P and S to S scattering is similar to acoustic scattering if the random medium consists of velocity fluctuations in that, at high frequencies, most of the energy is scattered forward. However, if the random medium consists of impedance fluctuations, most of the energy is backscattered at high frequencies.

In this report, we shall be dealing with scattered seismic waves that form the coda of local earthquakes. These waves arrive after the

the total scattering cross-section.

If ΔV in (4) is taken as a slab consisting of a unit area face in the plane of the wavefront and a side Δx perpendicular to the wavefront

$$\Delta I_I = -G(f) \cdot I_I \cdot \Delta x \tag{6}$$

If we consider the wave to propagate through a scattering medium that may be split up into such slabs, (6) can be integrated (Wu, 1982) to obtain

$$I_I = I_0 \exp[-G(f)x] \tag{7}$$

This may be expressed formally in terms of a scattering Q, Q_s, if Q_s is defined by

$$I_I = I_0 \exp[-2\pi fx/(Q_s C)] \tag{8}$$

where C is the sound velocity. Then

$$1/Q_s = G(f)C/(2\pi f) \tag{9}$$

If the medium also attenuates anelastically, parameterised by an intrinsic Q, Q_I, then the total Q will be given by (Dainty, 1981)

$$1/Q = 1/Q_I + 1/Q_s \tag{10}$$

$$= 1/Q_I + G(f)C/(2\pi f) \tag{11}$$

The frequency dependence expected for Q_s may be deduced from the results presented earlier for a rigid, immovable sphere. For low frequencies Rayleigh scattering occurs; generally, G(f) has a similar frequency dependence as $g(\pi,f)$, that is to say, G(f) increases with frequency as f^4 leading to $Q_s \propto 1/f^3$. For high frequencies, the wavelength will be short and geometrical scattering may occur. Then G(f) will be independent of frequency and $Q_s \propto f$. Dainty (1981) has examined two cases of shear wave Q in which this may be true for frequencies above 1 Hz in the lithosphere. Dainty (1984) and Wu (1982) discuss the frequency dependence expected for Q_s when the scattering medium is characterised as a random medium rather than by discrete scatterers. Dainty (1984; included as Appendix 2 of this report) demonstrated that if there is a length scale associated with the random medium, and discontinuities within the medium, then at high frequencies (wavelength shorter than the length scale) the frequency dependence of $g(\theta,\phi,f)$ and G(f) will be the same as that for geometrical scattering, i.e., independent of frequency.

The theory presented so far is for the acoustic case. Wu and Aki (1984) have presented results for the elastic case. They find that, in addition to P to P and S to S scattering, which are analogous to acoustic scattering, there is also P to S and S to P scattering ("mode conversion"). However, there are no backscattered mode conversions (i.e., scattered back directly along the ray path). P to P and S to S scattering is similar to acoustic scattering if the random medium consists of velocity fluctuations in that, at high frequencies, most of the energy is scattered forward. However, if the random medium consists of impedance fluctuations, most of the energy is backscattered at high frequencies.

In this report, we shall be dealing with scattered seismic waves that form the coda of local earthquakes. These waves arrive after the latest direct arrivals, are incoherent between components, and are believed to be either backscattered surface waves or backscattered S waves (Aki and Chouet, 1975). The geometry of the backscattered paths considered in this model is shown in Figure 2. If times are long enough the source and receiver may be considered to be coincident. The source pulse is considered to be short and equivalent to the S wave pulse. Only single scattering is considered. The theory for this case is given in Aki and Chouet (1975) and Appendix 1 attached to this report. For S to S scattering in a medium of average velocity V (three dimensional spreading), the power spectrum as a function of time t is given by:

$$P(f,t) = A_b(f)t^{-2} \exp[-2\pi ft/Q] \tag{12}$$

$$A_b(f) = S^2(f) \cdot \exp[2\pi ft_s/Q] \cdot 8\pi V \cdot g\ (\pi,f) \cdot t_s^2 \tag{13}$$

S(f) is the Fourier transform of the S wave pulse, t_s is the travel time of the direct S wave, $g(\pi,f)$ is the S to S backscattering turbidity and Q is given by (10) or (11). For the case of surface wave scattering (two dimensional spreading),

$$P(f,t) = A_s(f)t^{-1} \exp[-2\pi ft/Q'] \tag{14}$$

$$A_s(f) = [S'(f)]^2 \cdot \exp[2\pi ft_s'/Q'] \cdot 2\pi V' \cdot g'(\pi,f) \cdot t_s' \tag{15}$$

The primed variables in (14) and (15) have the same definitions as before, but for surface waves rather than for S waves. The results discussed in this report will be interpreted using (12) and (14).

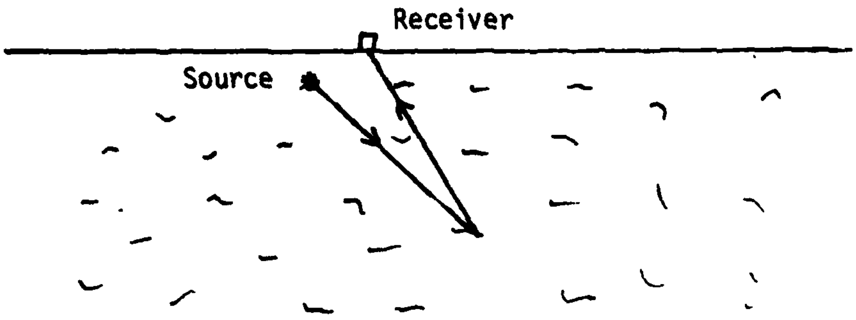

Figure 2. Ray path geometry for coda waves (three-dimensional spreading)

Summary of Analysis and Results

The basic data base consists of digital seismograms of local earthquakes. Five sets of seismograms were available. Four of these sets were taken by the United States Geological Survey, or using their equipment, and consist of sampled time series of three component data with a sampling interval of 0.005 sec. These sets were taken at Mammoth Lakes, California; Morgan Hill, California; Monticello, South Carolina; and New Brunswick, Canada. The fifth set consists of digital seismograms taken by the Eastern Canadian Network, McKendrick Lake Station, vertical component only, recorded at a sampling interval of 60 samples per second. Procedures for analysing the data according to equations (12) or (14) have been presented in Duckworth and Dainty (1983), included in this report as Appendix 1. Briefly, one component of the seismogram is Fourier transformed in a sliding window and the average Fourier amplitude as a function of time determined. Equation (12) or (14) is then fitted to the coda at times greater than twice the S wave travel time, estimated, together with the origin time, from the S-P times. The S wave Fourier amplitude is also determined by taking the average of the two nearest windows; the window length (usually 1.28 sec) was chosen to correspond roughly to the S pulse length. Then the two unknown parameters, Q and $g(\pi,f)$ (or their primed equivalents), were determined.

Preliminary results obtained by Duckworth and Dainty (1983) indicated that Q was approximately proportional to frequency over the frequency range 3-50 Hz. This suggests attenuation primarily by geometrical scattering (see Dainty, 1984, Appendix 2). Accordingly, to compare Q and $g(\pi,f)$, a quantity called the apparent total turbidity is calculated from

$$G_a(f) = 2\pi f/(QV) \tag{16}$$

V in this report is taken to be 3.2 km/sec, typical of shear/surface wave velocities in the upper crust. If anelastic attenuation can be neglected, $G_a(f)$ will be equal to $G(f)$. Otherwise,

$$G_a(f) > G(f) > g(\pi,f) \tag{17}$$

The last inequality follows from (3) and (4).

In attempting to fit codas from Monticello, South Carolina, it was found that a single value of A_b (or A_s) and $G(\pi,f)$ (or $G'(\pi,f)$) did not provide a good fit to codas of total duration longer than 10 seconds; there appeared to be a change in the decay rate of the coda at this time (see Appendix 1 for an example). For these codas, separate fits were made of the coda before 10 seconds and the coda after 10 seconds. A similar effect was noted on the records from the Eastern Canadian Network station with the change in decay rate occurring at about 15 seconds. Since the McKendrick Lake station was 25 km from the aftershock area, meaning that the direct S travel time was about 7.5 seconds, it was not possible to fit the early coda and maintain the rule that only coda at times greater than twice the direct S travel time is used for the fit. However, the results from McKendrick Lake may be compared to results from the United States Geological Survey New Brunswick seismograms, which are in the same area and from the same aftershock sequence, but much closer. The U.S.G.S. seismograms are too short to cover the time frame beyond 15 seconds.

In fitting (12) or (14), only one component of data has been used, usually the vertical. Properly, the sum of the squared amplitude spectra for three components in each window should be used. However, three component data was not always available, so single component data was analysed so that results could be compared. This should not affect the measurement of $G_a(f)$, since the decay rate should be the same for all components provided that one is not examining different types of waves on different components, but the measurement of $g(\pi,f)$ could be affected. To test this, and to examine the effect of different components on estimation of $G_a(f)$, analyses of three component measurements carried out separately for each component are presented in Figure 3 for a Morgan Hill event and in Figure 4 for a New Brunswick event, using U.S.G.S. data in the frequency range 3-50 Hz. In both cases, the results for $G_a(f)$ are quite consistent for the three components, with the exception of the vertical in New Brunswick for the frequencies 3 and 6 Hz. The results for $g(\pi,f)$ are also, in the main, quite consistent. This indicates that sufficiently accurate results for our purposes may be found by analysing only a single component of the data; this considerably increases the amount of data that may be considered.

An implicit assumption made in this analysis is that the parameters $G_a(f)$ and $g(\pi,f)$ derived are characteristic of the region in which the measurements are taken and not the station or the event. This assumption was tested at the Mammoth Lakes, California, site, and the

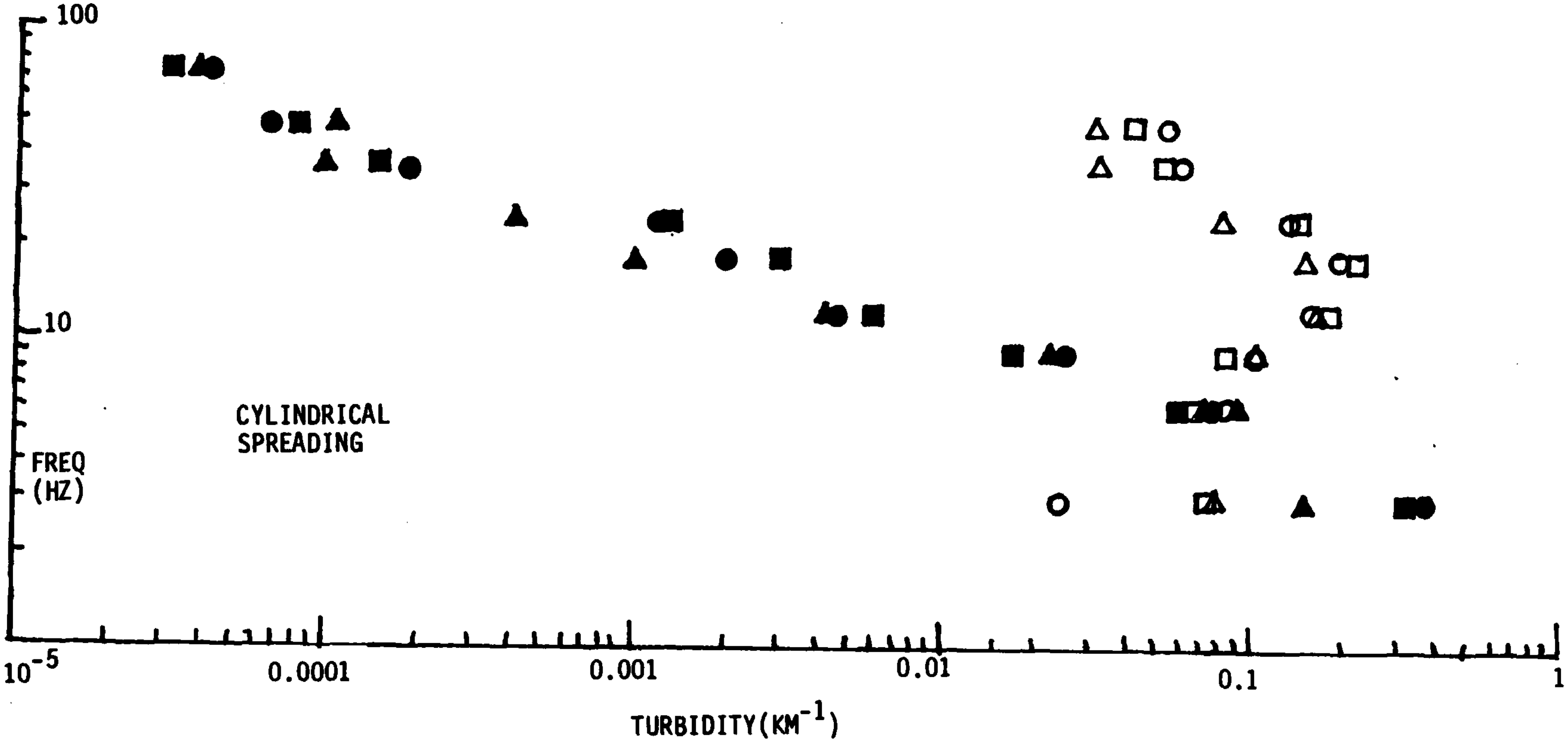

Figure 3. Total apparent turbidity (open symbols) and backscattering turbidity (closed symbols) for three components of event on 8 June, 1984, 17:48 UT at Morgan Hill, California. Circles, vertical component; triangles, North - South component; squares, East - West.

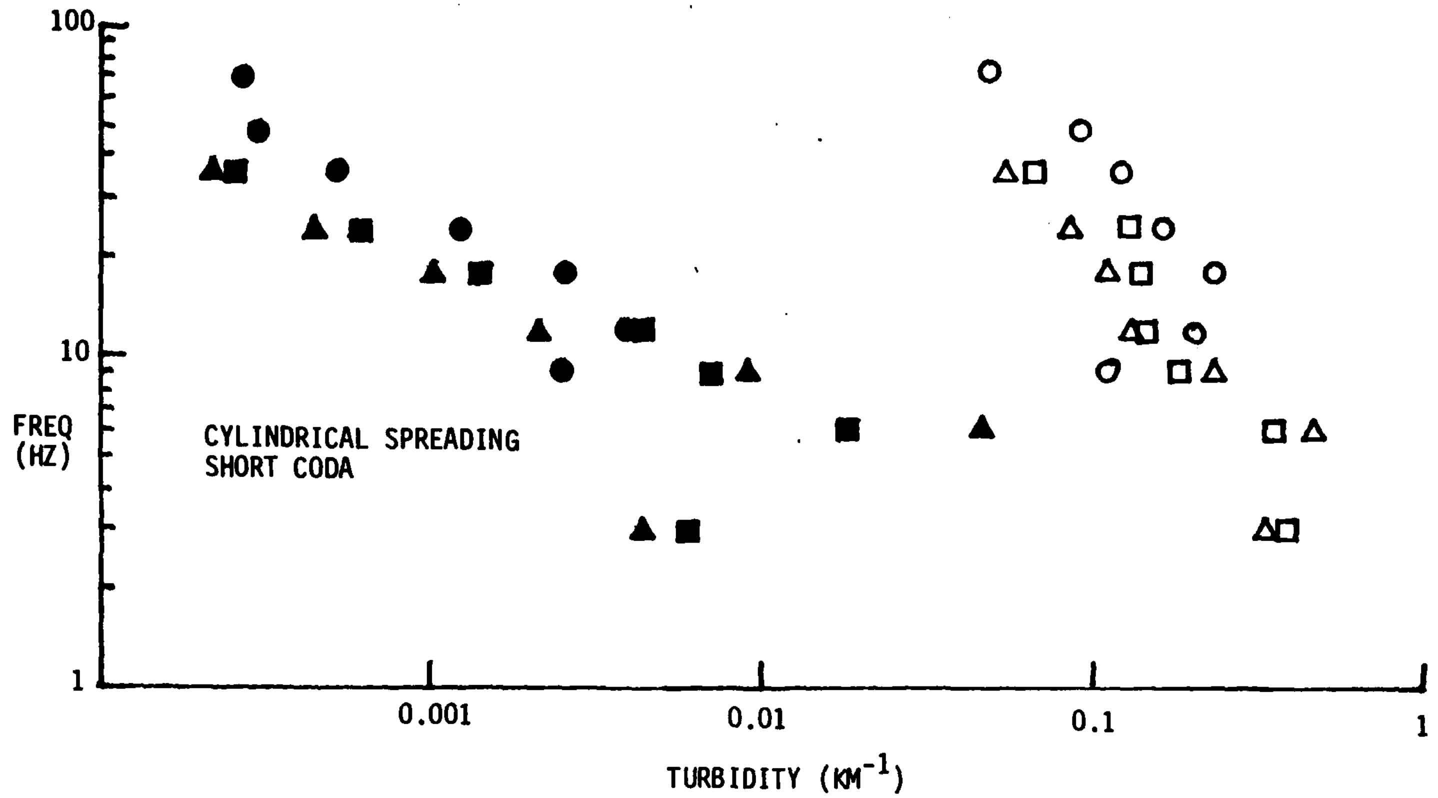

Figure 4. Total apparent turbidity and backscattering turbidity for three components of event on 17 January, 1982, 13:33 UT in New Brunswick, Canada. Symbols as for Figure 3.

results are shown in Figures 5 and 6. While there is considerable variation, the values are consistent, within an order of magnitude.

Typical results for Morgan Hill, California, and New Brunswick, Canada (codas less than 15 seconds long), have already been shown (Figures 3 and 4), using equation (14) (cylindrical spreading). Figure 7 shows typical results from New Brunswick, Canada (codas more than 15 seconds long), again using equation (14). Figures 8, 9, and 10, taken from Dainty (1984), show averaged results for, respectively, Monticello, South Carolina (codas less than 10 seconds long); Monticello, South Carolina (codas more than 10 seconds long); and Mammoth Lakes, California.

Discussion

From Figures 3, 4, 7, 8, 9, and 10, the codas examined here may be divided into two cases. Figures 7 and 9 show the results from long codas in eastern North America (Monticello, South Carolina, and New Brunswick, Canada), a non-tectonic area. The values of $G_a(f)$ are mostly between 0.005 and 0.05 km^{-1}, and the values of $g(\pi,f)$ are between 0.0001 and 0.002 km^{-1}, substantially less than most of the corresponding values in Figures 3, 4, 8, and 10. Also, in fitting (12) and (14) to the data, negative values of Q (and $G_a(f)$) were often obtained for (12) (spherical spreading). This is indicated in Figure 7 (Monticello data) for frequencies of 6, 9, and 12 Hz; for the New Brunswick data, Q was negative for 3 Hz, infinite for 6 Hz, and very high for the two higher frequencies. From (12), a negative Q means that the coda power spectrum decays less rapidly than t^{-2}. This probably means that these long

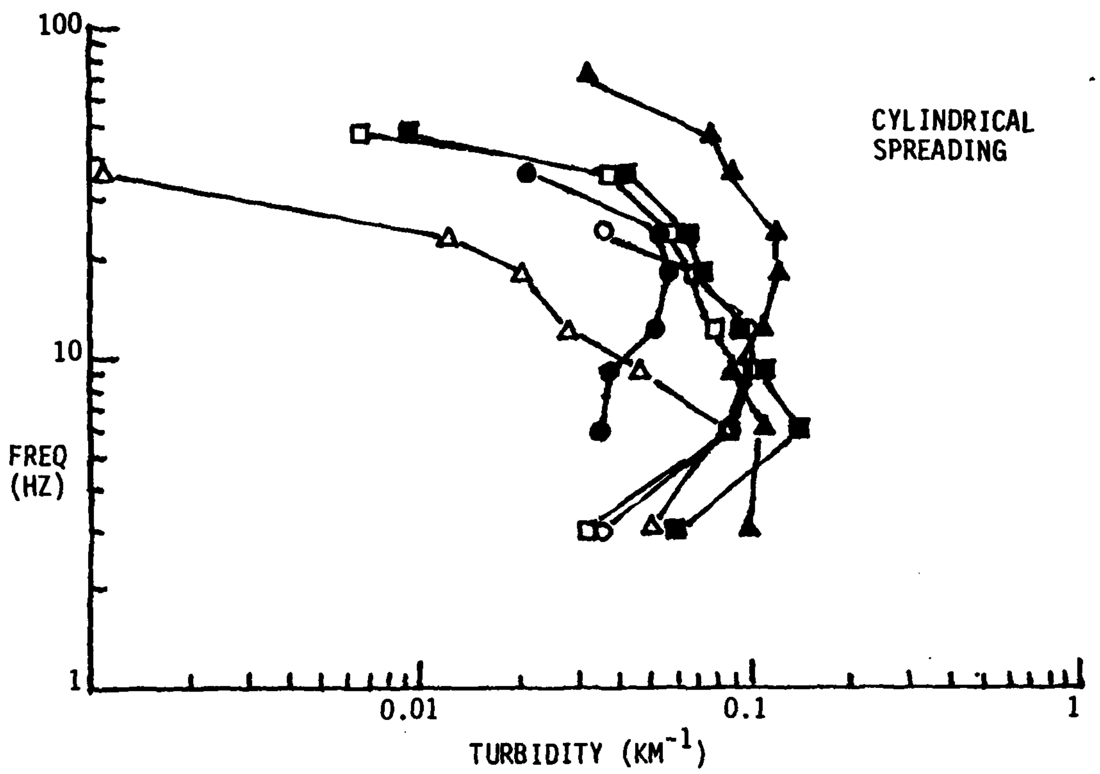

Figure 5. Total apparent turbidity for events 1571941 (open symbols) and 1592317 (closed symbols) at Mammoth Lakes, California (see Appendix 1 for details of events and stations). Open circle, station CBR; open triangles, LKM; open squares, TOM; closed cicles, LAK; closed triangles, ROC; closed squares, TOM. Results above 30 Hz probably not reliable.

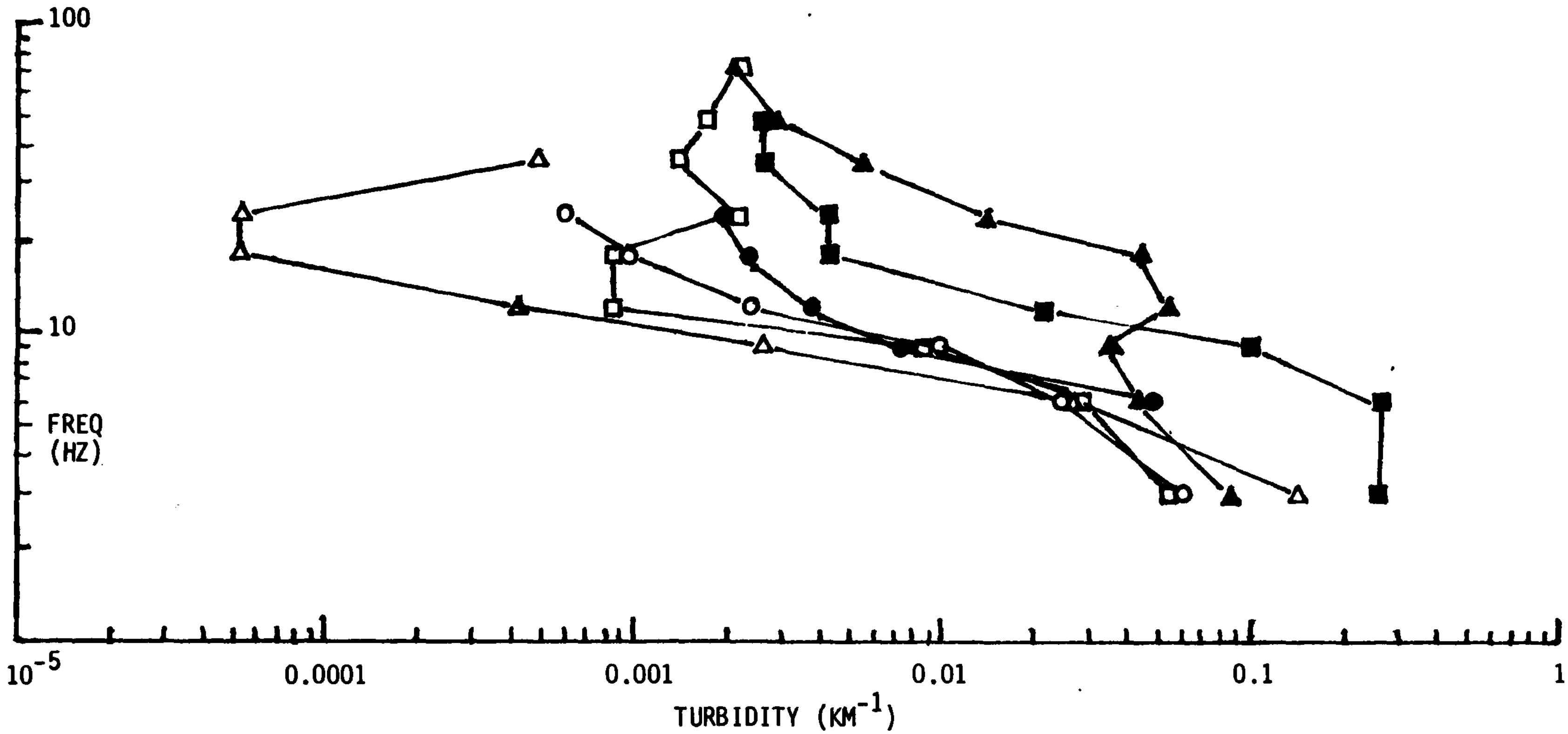

Figure 6. Backscattering turbidity, same events, stations and symbols as for Figure 5.

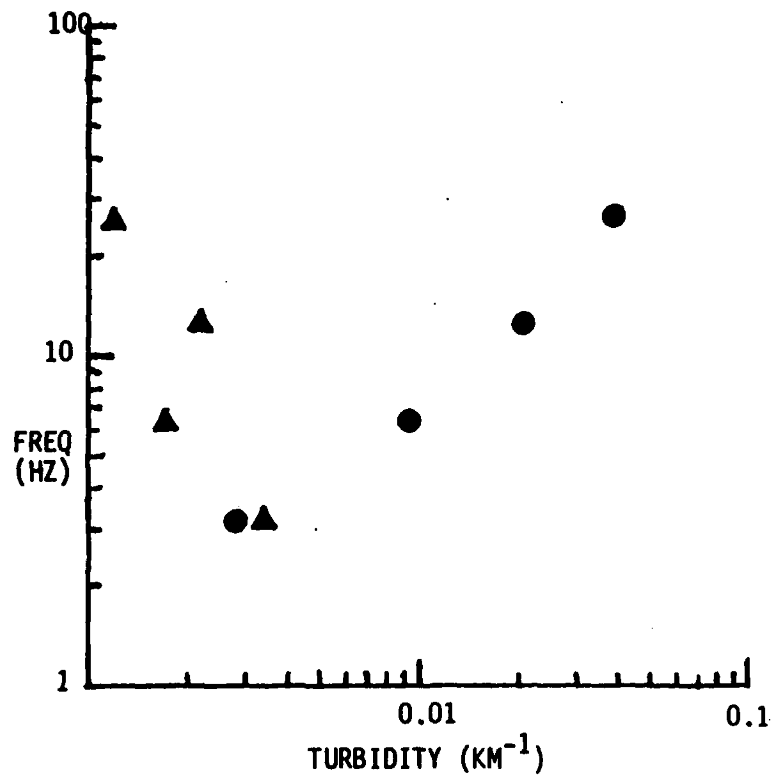

Figure 7. Total apparent turbidity (circles) and backscattering turbidity (triangles) for event on 20 March, 1982, 3:7 UT in New Brunswick, Canada, recorded at McKendrick Lake. Long coda, clyndrical spreading.

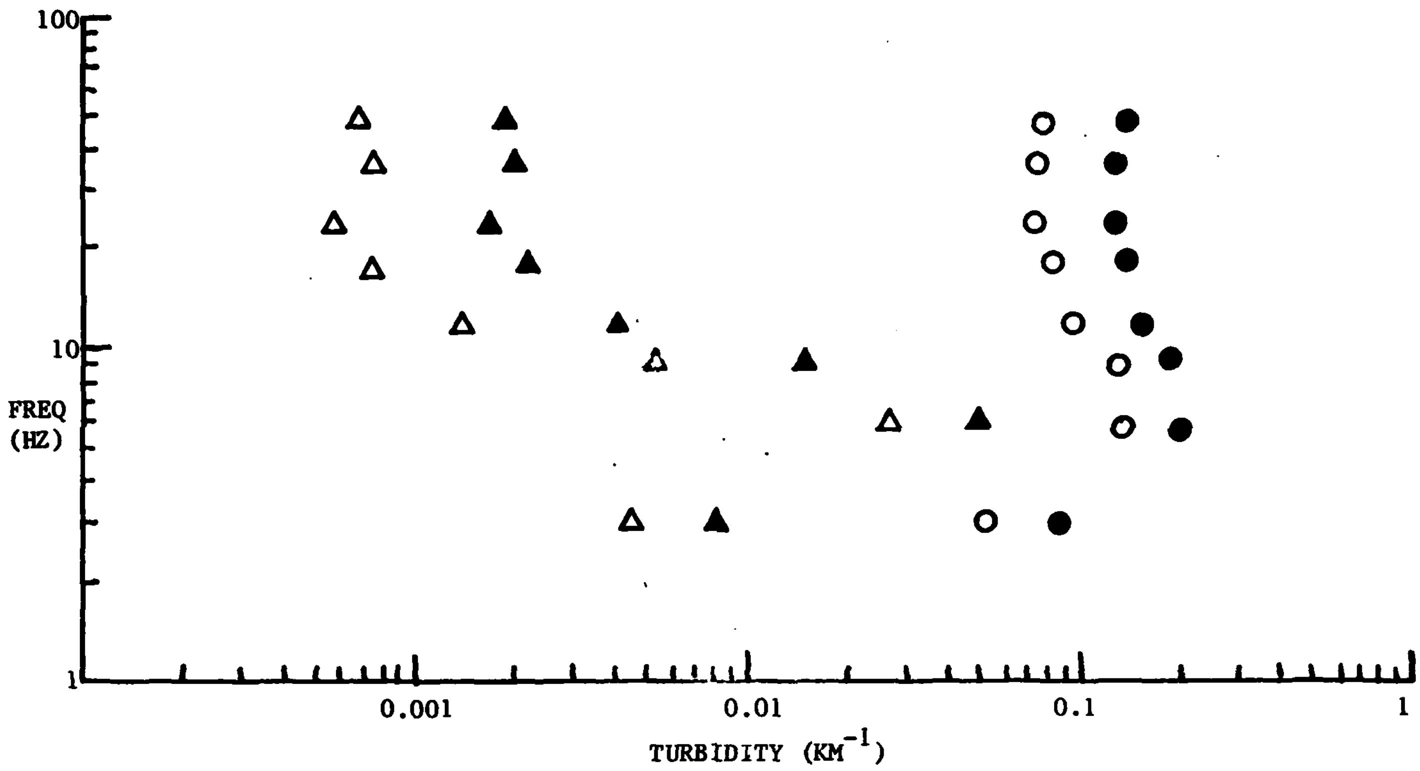

Figure 8. Total apparent turbidity (G_a) and backscattering turbidity ($g(\pi,f)$) as a function of frequency, Monticello, SC, for codas less than 10 seconds long. Open symbols, spherical spreading assumed, closed symbols, cylindrical spreading assumed. Circles are G_a, triangles are $g(\pi,f)$.

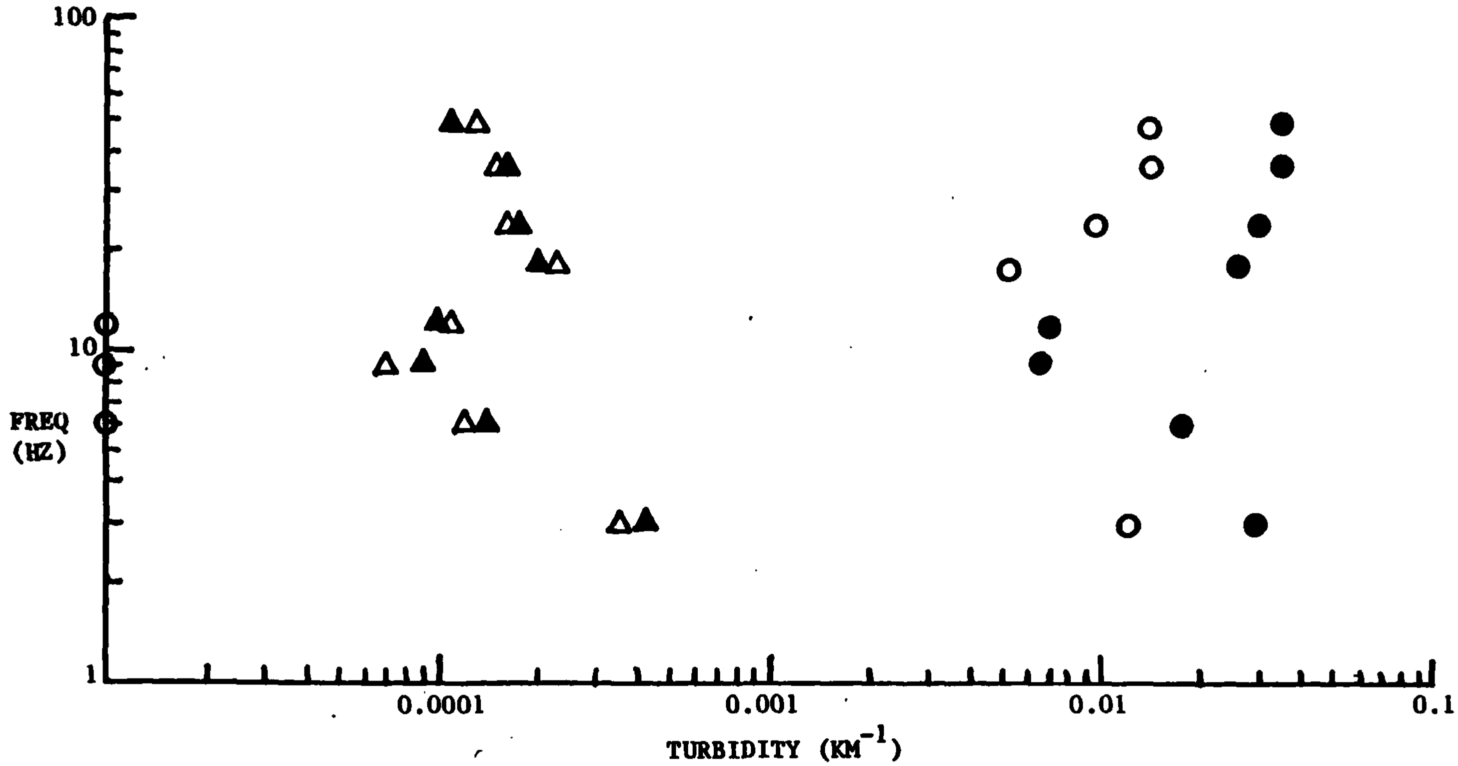

Figure 9. Total apparent turbidity and backscattering turbidity as a function of frequency, Monticello, SC, for codas more than 10 seconds long. Symbols as for Figure 8.

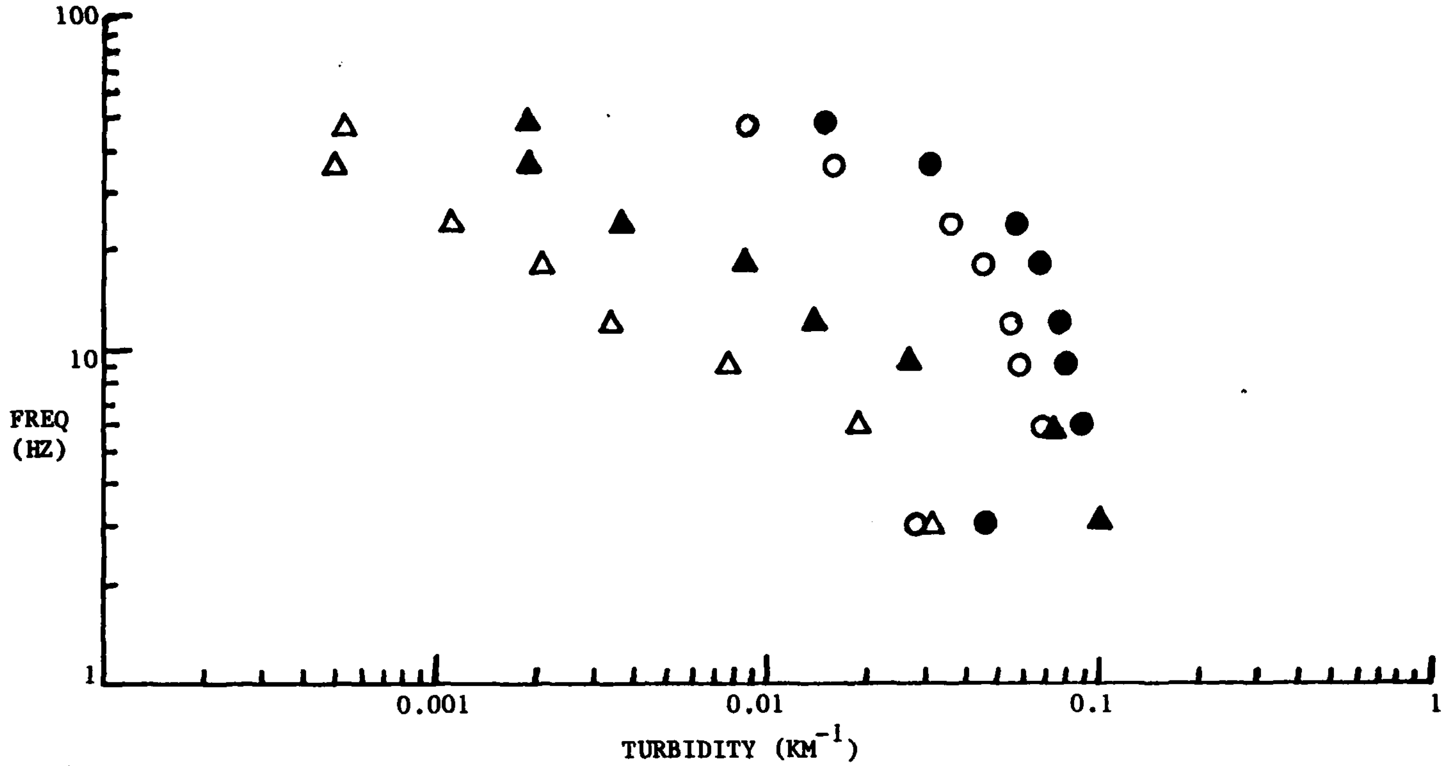

Figure 10. Total apparent turbidity and backscattering turbidity, Mammoth Lakes, CA, for codas more than 10 seconds long. Symbols as for Figure 8.

codas consist of energy that is at least partially "channeled" horizontally, like an Lg wave. This in turn implies that measurements on such codas (long means longer than 10 or 15 seconds; this is in fact the usual situation) would probably give a good estimate of Lg Q (Mitchell and Nuttli, 1983; Pomeroy and Peseckis, 1984). Also, it confirms the importance of scattering in Lg propagation (Gupta and Blandford, 1983).

The short codas (less than 10 or 15 seconds long) in eastern North America (New Brunswick, Figure 4; Monticello, Figure 8) and <u>all</u> the codas, long or short, in California (Morgan Hill, Figure 3; Mammoth Lakes, Figure 10) have higher rates of decay, as shown by values of $G_a(f)$ of around 0.1 km^{-1} and generally higher values of $g(\pi,f)$, between 0.005 and 0.1, than the long codas.

The separation of long and short codas may be explained in two ways. One possibility is that, in the case of the eastern North America codas, there are two modes of propagation, one of them ("short codas") more highly scattered (higher $G_a(f)$ <u>and</u> $g(\pi,f)$) than the other. The more highly scattered mode will dominate at short times, since $g(\pi,f)$, which controls the excitation of the coda, is larger, but the faster decay of this mode means that the mode with the smaller value of $G_a(f)$ (higher Q, by (16)) will dominate at long times. In California, either the second mode is not present or its scattering characteristics are similar to those of the first mode. If the identification of the long coda mode in eastern North America with waves similar to Lg is correct, the absence or greater scattering of such waves in California implies that Lg would not propagate as well in California as in eastern North America, in agreement with observation (Nuttli, 1973).

A second possibility is that the change in coda characteristics at Monticello and New Brunswick is due to a change from single scattering to multiple scattering at 10-15 seconds time. Sato (1977) gives

$$t > 1/(GV) \tag{18}$$

as a necessary but not a sufficient condition for multiple scattering. If $G \sim 0.1\ km^{-1}$, a typical value for the short codas, then (18) is met for $t > 3$ sec. Also, for the extreme case of very strong scattering, seismic energy in the coda will diffuse (Dainty and Toksöz, 1977), and an appropriate formula for the coda power spectrum in a three-dimensional medium is

$$P(f,t) = E(f)t^{-3/2} \exp[-3R^2G/(4Vt)] \exp[-2\pi ft/Q_i] \tag{19}$$

$$\rightarrow E(f)t^{-3/2} \exp[-2\pi ft/Q_i] , \quad R^2/t \rightarrow 0 \tag{20}$$

$$E(f) = S^2(f) ; \sqrt{27G^3} / (8\sqrt{\pi^3V^3}) \tag{21}$$

R is the source-receiver distance, taken to be small in (20). Like (12) and (14), (20) has the form of an inverse power law times an exponential, but the exponential contains only the intrinsic attenuation Q_i, not Q defined by (11). Accordingly, a change in decay rate to lower values would be expected if the coda changed from a single scattering phenomenon to a multiple scattering phenomenon. Finally, we note that for short codas at frequencies less than 10 Hz, relation (17) is often not met, at the same time that $G_a(f)$ is decreasing relative to its value at higher frequencies. This is a strong indication that multiple scattering is occurring in the short codas, and that the values of $G_a(f)$ obtained by fitting (12) or (14) are too low.

In spite of these indications that multiple scattering is occurring in the short codas, the suggestion that the change from short to long codas reflects a change from single to multiple scattering is rejected for the following reasons. First, all of the arguments in favor of multiple scattering in the eastern United States apply with equal force to California, yet the change in coda is not observed there. Thus, there must be regional differences. Furthermore, if condition (18) is applied with $G \sim 0.01\ km^{-1}$, a typical value for the Monticello codas, then single scattering would be expected for $t < 30$ sec, which is the typical length of one of these codas. For these Monticello codas, condition (17) is also met, although not at 3 Hz for the New Brunswick codas.

The nature of the scatterers and the contribution of scattering to attenuation may be partially answered from the data presented here. For the long codas at Monticello, there is a good correlation between $G_a(f)$ and $g(\pi,f)$, particularly around 10 Hz. For all codas except the long Monticello codas, there is a good evidence that scattering is strong for frequencies below about 10 Hz, which would indicate a substantial contribution to attenuation through (10) or (11). In cases below 10 Hz where multiple scattering is believed to be occurring, $G_a(f)$ declines relative to higher frequencies, again indicating that a substantial part of the attenuation is due to scattering, from (11), (16), and (20). Finally, as pointed out earlier, $G_a(f)$ is approximately constant with frequency, in the main, implying Q proportional to frequency; this is characteristic of attenuation by geometrical scattering. For these reasons, we estimate that at least 50% of the attenuation observed in the crust is due to scattering.

The nature and location of the scatterers may be partly determined from the data presented here. In cases where single scattering is believed to be occurring, i.e., long Monticello codas, and other codas at high frequencies (>10 Hz), $g(\pi,f)$ is about 1% of $G_a(f)$; this is typical of velocity fluctuations in a three dimensional medium (Wu and Aki, 1984; Dainty, 1984, Appendix 2), although it is not clear what would happen in a two dimensional case. Since the events range from 0 to 10 km depth, the short codas must be at least partially due to scatterers in the upper crust, since these codas start immediately after the direct S pulse. The long codas start at 10-15 seconds, which implies a mid to upper crust propagation, since the scattered wave has to get to the scatterer from the source and back in 10-15 seconds at $\sim$3.2 km/sec.

The principal remaining question with the codas studied here is whether horizontal channeling of energy (two dimensional spreading, (14)) as opposed to spherical spreading (12) is the mode of energy propagation. For the long codas, evidence has been offered that horizontal channeling is occurring; for the short codas, the question is open. Note that for horizontal channeling, more than surface waves, sensu strictu must be involved, since the skin depth of surface waves at, say, 10 Hz is a few hundred meters, less than the focal depth of many of the events. Generally, the decomposition of codas into waves of different types is a major remaining problem.

What is the significance of these results for the estimation of seismic yield? First, they illustrate that scattering occurs in the upper part of the crust, where the source and the receiver are located, and this scattering has a significant effect on attenuation. For example, if $G_a(f)$ is 0.1, then on travelling through 10 km of such material, the energy in a short pulse will be down by 1/e. This is equivalent to about 0.2 on the m_b magnitude scale, which uses measurements at frequencies ($\sim$1 Hz) close to those investigated here (3-50 Hz). If the scattering effect varied from place to place, this could introduce bias of the order of tenths of a magnitude point, which is significant. Further, if $G_a(f)$ is independent of frequency over some frequency range, as has been observed in this study, then the attenuation effect could not be detected by spectral ratio methods within that frequency range.

This study also indicates that the attenuation of the regional phase Lg should vary from region to region, being low in regions wimilar to eastern North America, a non-tectonic region, and high in regions similar to California, a tectonic region, in accord with observations (Nuttli, 1973). A good estimate of this attenuation should be obtainable from the coda after 10 seconds (Mitchell and Nuttli, 1983).

Three questions for further investigation suggest themselves: Can the scattering characteristics derived for a region from local codas be found from teleseismic observations, such as teleseismic P codas? Could a region be "calibrated" in terms of the scattering attenuation of teleseismic phases by observations of local coda? What other effects does scattering have on the waveforms of short pulses?

Acknowledgments

Paul Spudich of the United States Geological Survey, Menlo Park, kindly supplied the seismograms for Mammoth Lakes, California, and Monticello, South Carolina. Chuck Mueller of the same organization supplied the "short" seismograms for New Brunswick, Canada. Ralph Archuleta and Gene Sembera, also of the above organization, graciously allowed us to use their instruments to collect data from Morgan Hill, California. The data from the Eastern Canadian Network for New Brunswick, Canada, was supplied by Bill Shannon, of the Department of Energy, Mines and Resources, Government of Canada.

Bibliography

Aki, K., and B. Chouet (1975). Origin of coda waves: Source, attenuation, and scattering effects. J. Geophys. Res., 80, 3322.

Chernov, L. A. (1960). Wave Propagation in a Random Medium. McGraw-Hill, New York.

Clay, C. S., and H. Medwin (1977). Acoustical Oceanography. John Wiley, New York.

Dainty, A. M. (1981). A scattering model to explain seismic Q observations in the lithosphere between 1 and 30 Hz. Geophys. Res. Lett., 8, 1126.

Dainty, A. M. (1984). High frequency acoustic backscattering and seismic attenuation. J. Geophys. Res., 89, 3172.

Dainty, A. M., and M. N. Toksoz (1977). Elastic wave propagation in a highly scattering medium--a diffusion approach. J. Geophys., 43, 375.

Duckworth, R. M., and A. M. Dainty (1983). Observations of coda Q for the crust near Mammoth Lakes, California, and Monticello, South Carolina. Semi-annual Technical Report No. 1, Contract AFOSR-83-0037.

Gupta, I. N., and R. R. Blandford (1983). A mechanism for the generation of short-period transverse motion from explosions. Bull. Seis. Soc. Am., 73, 571.

Mitchell, B. J., and O. W. Nuttli (1983). Attenuation of seismic waves at regional distances. Semi-annual Technical Report No. 1, Contract F49620-83-C-0015.

Nuttli, O. W. (1973). Seismic wave attenuation and magnitude relations for eastern North America. J. Geophys. Res., 78, 876.

Pomeroy, P. W., and L. L. Peseckis (1984). The use of regional seismic waves for yield determination. Semi-annual Technical Report No. 1, Contract F49620-83-C-0017.

Sato, H. (1977). Energy propagation including scattering effects single isotropic scattering approximation. J. Phys. Earth, 25, 27.

Sato, H. (1982). Amplitude attenuation of impulsive waves in random media based on travel time corrected mean wave formalism. J. Acoust. Soc. Am., 71, 559.

Wu, R.-S. (1982). Attenuation of short period seismic waves due to scattering. Geophys. Res. Lett., 9, 9.

Wu, R.-S., and K. Aki (1984). Scattering of random waves by a random medium and small scale inhomogeneities in the lithosphere. Annual Technical Report, Contract F49620-82-K-0004.

APPENDIX 1

OBSERVATIONS OF CODA Q FOR THE CRUST NEAR MAMMOTH LAKES, CALIFORNIA, AND MONTICELLO, SOUTH CAROLINA

By Robert M. Duckworth and Anton M. Dainty

Introduction

The seismic Q of a material is a measure of the degree to which it attenuates the harmonic energy content of seismic waves passing through it. Seismic energy released by earthquakes and underground explosions propagates in the earth primarily in the form of elastic waves. To the extent that earth materials are not perfectly elastic the elastic waves will be attenuated. The energy at an initial time, E_0, and the energy E after elapsed time t are related to the Q by

$$E = E_0 \exp(-2\pi ft/Q) \tag{1}$$

where f is the frequency of the wave. Attenuation is proportional to the distance a wave travels, x, since $t = x/B$ where B is the speed at which the wave propagates. Therefore, knowledge of Q should be useful in predicting the expected amplitudes of seismic waves for yield estimation and other applications. However, because earth materials are inhomogeneous a prediction of seismic wave amplitude is complicated.

Inhomogeneities lead to reflections and refractions, or scattering, of seismic waves. Scattering by these inhomogeneities is an important part of the seismic trace recorded as a function of time. The first part of a seismogram of a local (within a few hundred km of the seismic recording station) earthquake is the Primary or P-wave. This is a compressional wave and travels at speeds up to about 8 km/s for local earthquakes. A second major feature is the Secondary or S-wave which is a shear wave and travels at speeds of about P-speed/$\sqrt{3}$. Between the P and S arrivals and following the S arrival additional waves arrive. Their amplitude decays in a generally exponential manner. Aki (1969) proposed that these waves are the result of scattering of surface waves by surface inhomogeneities. He gave them the name Coda [Latin: tail] waves. Later, Aki and Chouet (1975) considered body wave scattering. Also, scattering affects the attenuation of seismic waves in two ways. Energy is scattered out of the primary wave decreasing the apparent Q. Some of this scattered energy arrives at the receiver in the form of coda waves. The amplitude of these depends upon the scattering mechanism, characterised by the turbidity as described below, and the inelastic Q.

This report presents estimates of the apparent Q from the coda of local earthquakes in two different geologic regions. Attempts are made to separate the effects of scattering and inelasticity in order to determine the turbidity and inelastic Q for each region. The excitation of the coda has also been considered.

Theory

Coda waves are generally considered to be backscattered energy. A model from Aki and Chouet (1975) of coda waves as single, S-wave to

S-wave scatter from a random distribution of scatterers is used in this report.

Observations show the coda to be independent of source-receiver distance, R, for local coda waves (Aki, 1969; Aki and Chouet, 1975; Rautian and Khalturin, 1978). Sato (1977) lends support to this observation with a model for single isotropic scatter. He shows the time dependence of the mean energy density of the coda near the source to be nearly independent of source-receiver distance R for $R \ll Bt/2$. B is the velocity of S-waves in the medium and t is their travel time measured from the origin time. Because the coda shape is nearly independent of source receiver distance for local coda waves, the model is simplified to the case of coincident source and receiver.

Knopoff and Hudson (1967) modeled scatter from small perturbations in an elastic medium. They found the amplitude for S to S scatter to dominate that of P to P scatter by $(\alpha/B)^2$ for geometric (high frequency) and $(\alpha/B)^4$ for Rayleigh (low frequency) scatter and P to S and S to P scatter to be "vanishingly small" for geometric scatter. α and B represent the speeds of P and S waves respectively. For the crust $\alpha = \sqrt{3}\,B$ is a good approximation and the amplitude of S to S scatter is greater than P to P scatter by a factor of 3 for geometric scatter. The observed character of coda waves also supports S to S dominance (Aki, 1980).

Before presenting a model of coda waves the effects of attenuation will be considered. Plane waves traveling in a medium with a random distribution of scatterers will be attenuated. Let E_0 represent the average energy of the waves before scattering and E represent the energy of plane waves traveling in the same direction as the primary waves after scattering. We assume the primary cause of attenuation by scattering will be backscatter. For $(E_0-E) \ll E_0$ over a distance equal to the average separation of "backscatterers", the attenuation of primary waves is given by

$$E/E_0 = \exp(-x\rho\sigma_b). \qquad (2)$$

The backscatter cross section σ_b represents the average of the product of the backscatter function and the projected area of the scatterers, or the average apparent area of the scatterers. ρ is the number of scatterers per unit volume. As σ_b and ρ are unknown for the crust, their product is often replaced by a scattering coefficient, g, called the turbidity. The turbidity represents the fractional loss of energy due to scatter per unit distance traveled. The term was introduced by Chernov (1960) and first used in seismic literature by Galkin et al. (1970). They employ it to describe their observed high frequency spatial variation of seismic amplitudes as a function of distance from the source. Equation (2) may also be applied to the attenuation a plane wave suffers when passing through a medium where scattering is occurring as a result of random fluctuations in the medium properties rather than discrete "backscatterers". In this case, g is a function of the statistical properties of the medium and the wavelength (Wu, 1982).

In the earth medium there will also be attenuation resulting from inelasticity. This is attenuation that occurs as elastic energy is converted to heat. For $(E_0-E) \ll E_0$ over a wavelength, the inelastic attenuation is given by

$$E/E_0 = \exp(-2\pi fx/BQ). \qquad (3)$$

Q is the quality factor, B is the speed of shear waves, x is the distance they travel in the medium and f is frequency. The inelastic attenuation mechanism is not well understood. It is generally observed that Q is independent of frequency over the range of seismic frequencies studied. This is in agreement with the results of Knopoff (1964) who studied Q in the laboratory and found it independent of frequency for dry materials. These two attenuation effects can be combined. In terms of the time the energy spends in the medium $t = x/B$ and for constant B,

$$E/E_0 = \exp(-2\pi ft/Q) \,.\, \exp(-Btg) \qquad (4a)$$

$$= \exp[-t(2\pi f/Q_T)]. \qquad (4b)$$

Q_T represents the combined effects of scattering and inelastic attenuation.

$$1/Q_T = 1/Q_i + gB/2\pi f \;, \qquad (5)$$

where Q_i is the inelastic Q (Dainty, 1981). Dainty and Toksoz (1981) suggest that for a single scatter theory to apply $2\pi f/Q_i >> Bg$ is a necessary condition, as otherwise there would be sufficient energy for higher order scattering.

The power spectrum of the coda as a function of time under the conditions discussed above has been derived by Aki and Chouet (1975). If the spectrum of the source is $\phi(f|r_0)$ at a reference distance r_0

from the source, the coda power spectrum is

$$P(f|t) = st^{-2m} \exp(-2\pi ft/Q_T) \tag{6}$$

where

$$s = |\phi(f|r_o)|^2 \; 4m\pi r_o^{2m}(B/2)^{1-2m} \cdot g \tag{7}$$

s represents the source term, the turbidity $g = \rho\sigma_b$, and $m = 0.5$ for cylindrical (surface wave) or $m = 1.0$ for spherical (body wave) spreading. The source term, s, will in general depend on the scatterers through its dependence on g. The time t is measured from the origin time of the event.

The average coda amplitude at a particular frequency and time $A(f|t)$ is related to the power spectrum.

$$A(f|t) = [P(f|t)\Delta f]^{1/2} \tag{8}$$

Δf is the band width considered about f. Q_T can therefore be measured from the coda wave amplitude attenuation using equation (6). Sato (1977) points out the single scatter model is only applicable for a coda duration $t < 1/gB$. Longer times imply a significant contribution of higher order scattering which effects the return of scattered energy to the later parts of the coda. The decomposition of Q_T to find Q_i and g depends upon assumptions about their frequency dependence. This and the applicability of the single scatter model will be considered in the section on results.

Data

Two sets of earthquake data are available for analysis courtesy of Paul Spudich (U.S. Geological Survey at Menlo Park, California). Both sets contain digital records of earthquakes and their locations. Program Hypoinverse by Klein (1978) is the method of location. Locations and primary S-wave travel times of the earthquakes selected for analysis have been read from the U.S.G.S. tapes (Tables 1 and 2). The first set is from a series of events associated with the filling of Monticello Reservoir in South Carolina. It contains records of 32 earthquakes, recorded in May and June of 1979 and used in a study of stress drops by Fletcher (1982). He reports they are all magnitude $M < 1.7$. Secor _et al_. (1982) report the earthquakes as occurring in a heterogeneous quartz monzonite pluton of Carboniferous age. Zoback and Hickman (1982) suggest that the earthquakes are shallow, occurring along existing fractures, and the result of an increase in pore pressure caused by increasing the head at the reservoir. Figure 1 adapted from Talwani and Hutchenson (1982) shows the location of the seismic stations and the reservoirs. Epicenters for the earthquakes considered have been indicated on this figure. They are all within 8 km of the recording stations. Secor _et al_. (1982) report on the two reservoirs. Parr Shoals reservoir was impounded in 1914 and increased in 1976 to a volume of 0.039 km^3 with a surface area of 18 km^2 and a maximum depth of 11 meters. Monticello reservoir has a volume of 0.5 km^3, a surface area of 27 km^2, and a maximum depth of 48 meters.

Fletcher (1982) describes the instrumentation used to record the Monticello earthquakes. A summary is given here. Sprengnether

Table 1. Locations of earthquakes and recording stations at Monticello, South Carolina.

EVENT/STATION	"S" TIME	RANGE	LOCATION
1271000			34 20.03 N 081 19.62 W
DUC	0.68	2.2	34 20.07 N 081 21.06 W
DON	1.05	3.5	34 21.42 N 081 21.20 W
LKS	0.89	3.0	34 19.95 N 081 17.69 W
1320218			NOT POSSIBLE
JAB	1.66	5.8	34 22.28 N 081 19.47 W
1281119			34 20.70 N 081 20.81 W
JAB	1.31	4.6	
1302328			34 20.49 N 081 20.65 W
SNK	0.56	1.8	34 20.29 N 081 19.54 W
JAB	1.19	3.8	
LKS	1.38	4.7	
1310603			34 18.50 N 081 20.50 W
SNK	1.05	3.7	
LKS	1.48	5.2	
JAB	2.00	7.0	
1281831			NOT POSSIBLE
JAB	1.02	3.57	

Table 2. Locations of Earthquakes and Recording Stations at Mammoth Lakes, California.

EVENT/STATION	"S" TIME	RANGE	LOCATION
1571941			37 32.91 N 118 52.53 W
MGE	3.17	8.0	37 33.67 N 118 47.22 W
HCF	4.37	10.6	37 38.51 N 118 50.98 W
CBR	5.50	15.2	37 40.75 N 118 49.51 W
TWL	4.84	13.7	37 36.93 N 119 00.37 W
ROC	5.67	14.9	37 29.78 N 118 43.16 W
TOM	6.11	18.0	37 33.05 N 118 40.32 W
LKM	5.97	17.3	37 41.80 N 118 56.13 W
1592317			37 37.50 N 118 52.52 W
HCF	2.38	3.0	
FIS	2.58	4.2	37 36.84 N 118 49.82 W
CBR	3.60	7.5	
LKM	3.73	9.6	
MGE	4.03	10.6	
TWL	4.52	11.6	
LAK	5.30	13.1	37 38.49 N 118 43.70 W
TOM	6.78	19.7	
ROC	6.71	19.8	

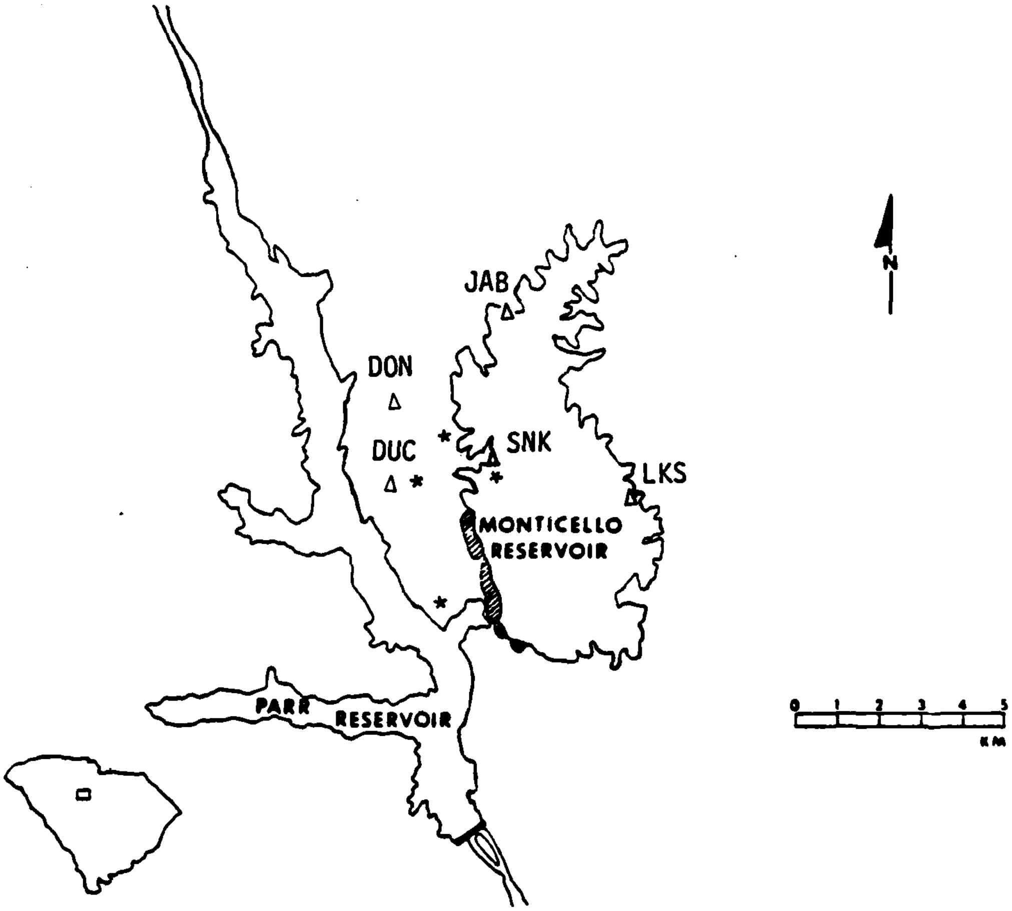

Figure 1. Recording Stations and Epicenters at Monticello Reservoir, South Carolina. stations(Δ), epicenters(*)

DR-100, 12-bit, digital recorders were used with an unspecified make of geophone. The sample rate was 200 Hz with an antialiasing filter of either 50 Hz or 70 Hz having a 30 db per octave rolloff. The geophones were velocity sensors with damping specified as 0.7 of critical. The possibility of aliasing on Monticello records for which the filter corner frequency was set at 70 Hz was considered. Inspection of bandpass filtered records at the higher frequencies revealed no difference in the rate of amplitude decay between the recordings made with a 50 Hz corner filter and a 70 Hz corner filter.

The second set of data is from Mammoth Lakes, California. It consists of the 150 earthquakes used by Archuleta et al. (1982) in a study of source parameters. The earthquakes followed a series of magnitude $M > 6.0$ earthquakes which occurred May 25, 1980 (Spudich et al., 1981). Wallace et al. (1982) investigate a discrepancy in fault plane projections as reported in the literature for the Mammoth Lakes earthquakes. Citing evidence of an active magma body, they suggest a low velocity zone related to recent magmatic activity as a possible cause. Figure 2 adapted from Spudich et al. (1981) shows the station locations. Epicenters for the earthquakes considered have been added to this figure. The source receiver distances range from 5 to 25 km. The Long Valley Caldera, a volcanic crater 0.7 million years old, is outlined along with major faults. The instrumentation at Mammoth Lakes is essentially the same as at Monticello, except that accelerometers are used at some of the Mammoth stations. Details of the instrumental operations and clock corrections can be found in Spudich et al. (1981).

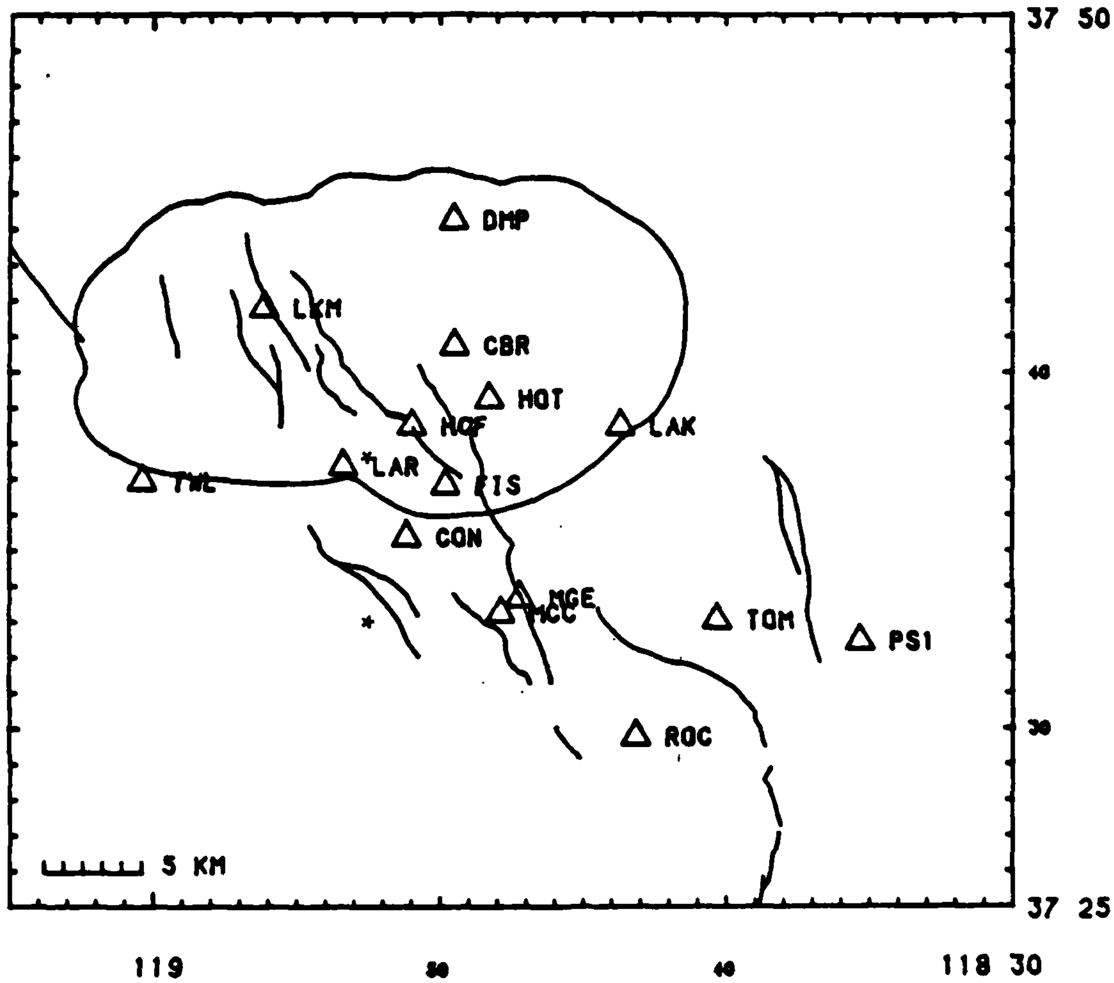

Figure 2. Recording Stations and Epicenters at Mammoth Lakes, California. stations(Δ), epicenters(*)

Analysis

The rms coda amplitude is related to the power spectrum by $A(f|t) = [P(f|t)\Delta f]^{1/2}$. Substituting the equation for the power spectrum in the single scatter model gives

$$A(f|t) = ct^{-m} \exp(-\pi ft/Q_T) \quad (9)$$

Over the range of frequencies for which geometric scatter is the case, σ_b is constant. Therefore, $c = (s\Delta f)^{1/2}$ has the same frequency dependence as the source for octave Δf. For cylindrical waves $m = 0.5$, while for spherical waves $m = 1.0$. Taking the ordinary logarithm of this expression

$$\log[A(f|t)] = C - m \cdot \log(t) - bt \quad (10)$$

is obtained where $b = \log(e)\pi f/Q_T$ and $C = \log(c)$. To estimate Q_T this equation is fit to filtered records by the method of least squares. This is the approach taken by Aki and Chouet (1975).

To study the temporal decay of coda waves the longest records are chosen. Of these the duration of recording ranges from 8.0 to 23.0 seconds at Monticello and from 10.0 to 35.0 seconds at Mammoth Lakes. Only a few records from Monticello are considered to be of sufficient duration for coda analysis (Table 1). The Mammoth Lakes records chosen for analysis are listed in Table 2.

Travel times are taken from the location data provided with the U.S.G.S. tapes. Some of the Monticello earthquakes were not located. For these the S-wave travel time is calculated from the difference in S and P wave arrival times and assumed S and P wave velocities of

3.5 km/s and 6.0 km/s respectively. Ground displacement amplitude as a function of time in octave wide bands is determined for the selected records by the following procedure.

The mean is removed from a record in a 256 sample (1.28 second) window centered about the origin time. This portion of the trace is multiplied by normalized Hamming coefficients. The windowed trace is corrected for instrument gain, Fourier transformed, and multiplied by $1/f$ or $1/f^2$. Assuming a flat instrument response in the frequency band of interest, this converts the trace to ground displacement amplitude from velocity and acceleration records respectively. It has been assumed, as in Archuleta et al. (1982) and Fletcher (1982), that the velocity response is flat from 2 Hz to 50 Hz and the acceleration response is flat above 0.1 Hz. The average amplitude is calculated within octaves (equal power bands) about selected center frequencies. The log of this amplitude is plotted at time zero on separate plots for each frequency. The window is then moved 100 samples (0.5 seconds) and the process is repeated with the log average amplitude plotted at time 0.5. This is done until the end of the record is reached. The result is a series of plots of log average amplitude versus time, measured from origin time, at selected center frequencies from 3 Hz to 72 Hz. Figure 3 contains a sample record and its corresponding filtered amplitude plots. Frequencies above the corner of the antialiasing filter are considered as the constant reduction in amplitude will only show up in the source term. Therefore Q_T can still be estimated provided there is sufficient energy present at these frequencies.

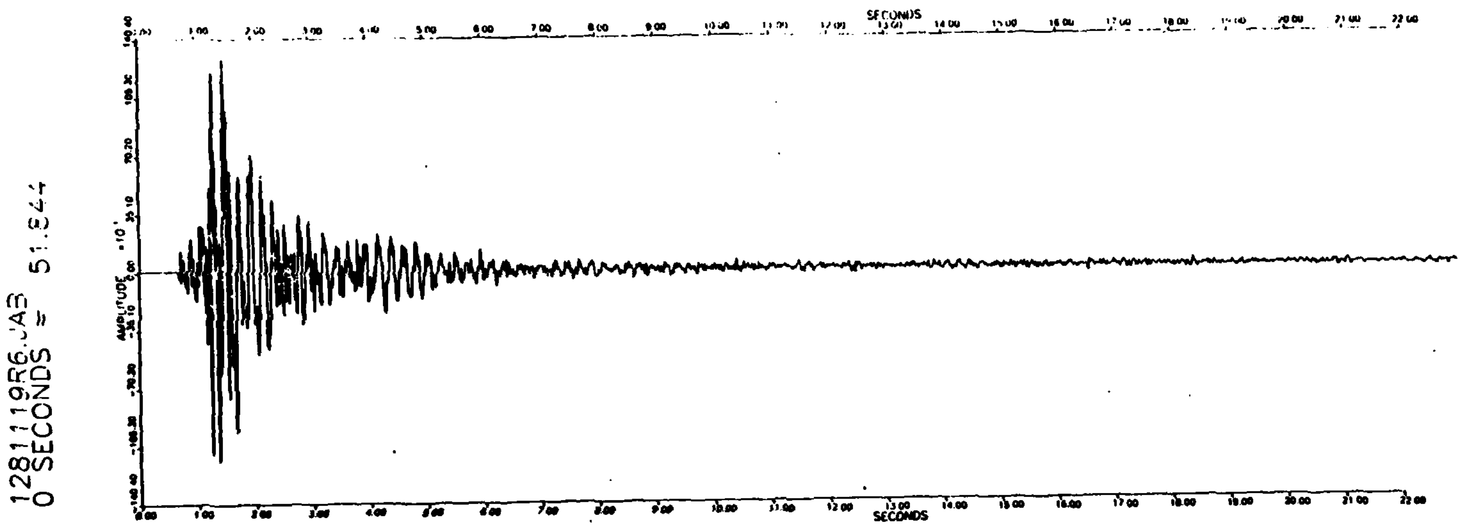

Figure 3a. Record of Event 1281119 at Monticello Reservoir. The amplitude scale is digitizing units.

Figures 3b-h. Log(amplitude) versus Time for Event 1281119at Monticello. (following 4 pages) Plots b-j correspond to center frequencies of 3, 6, 9, 12, 18, 24, 36, 48, and 72 Hz respectively. It can be seen from the coda that Q is changing with time. The early coda amplitude falls off rapidly while the late coda shows little decay.

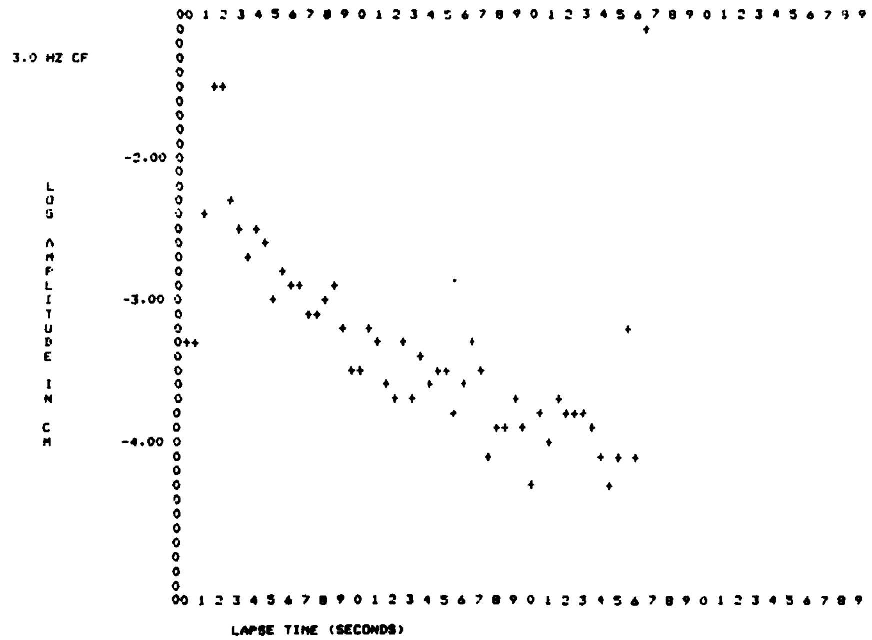

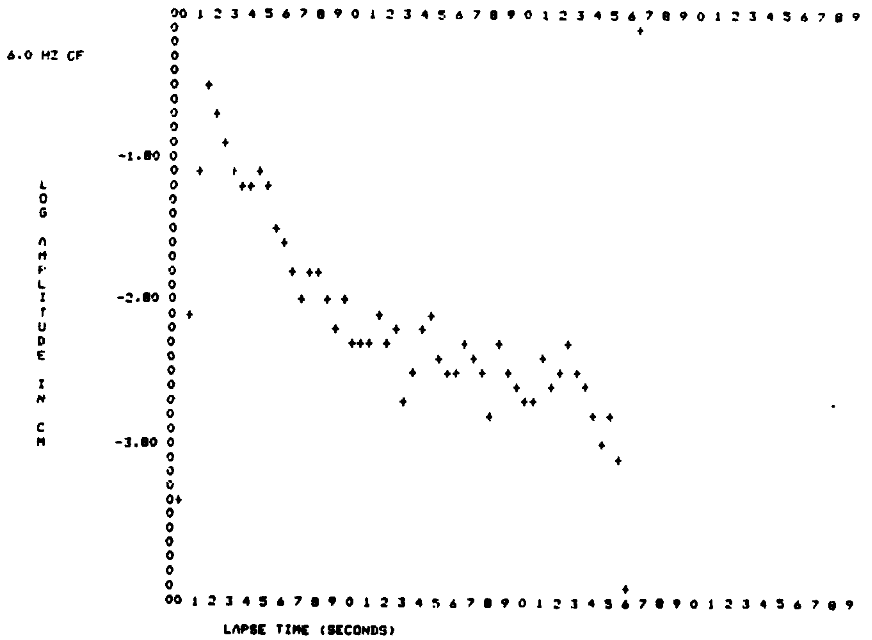

Figure 3 . b.(top). c.(bottom)

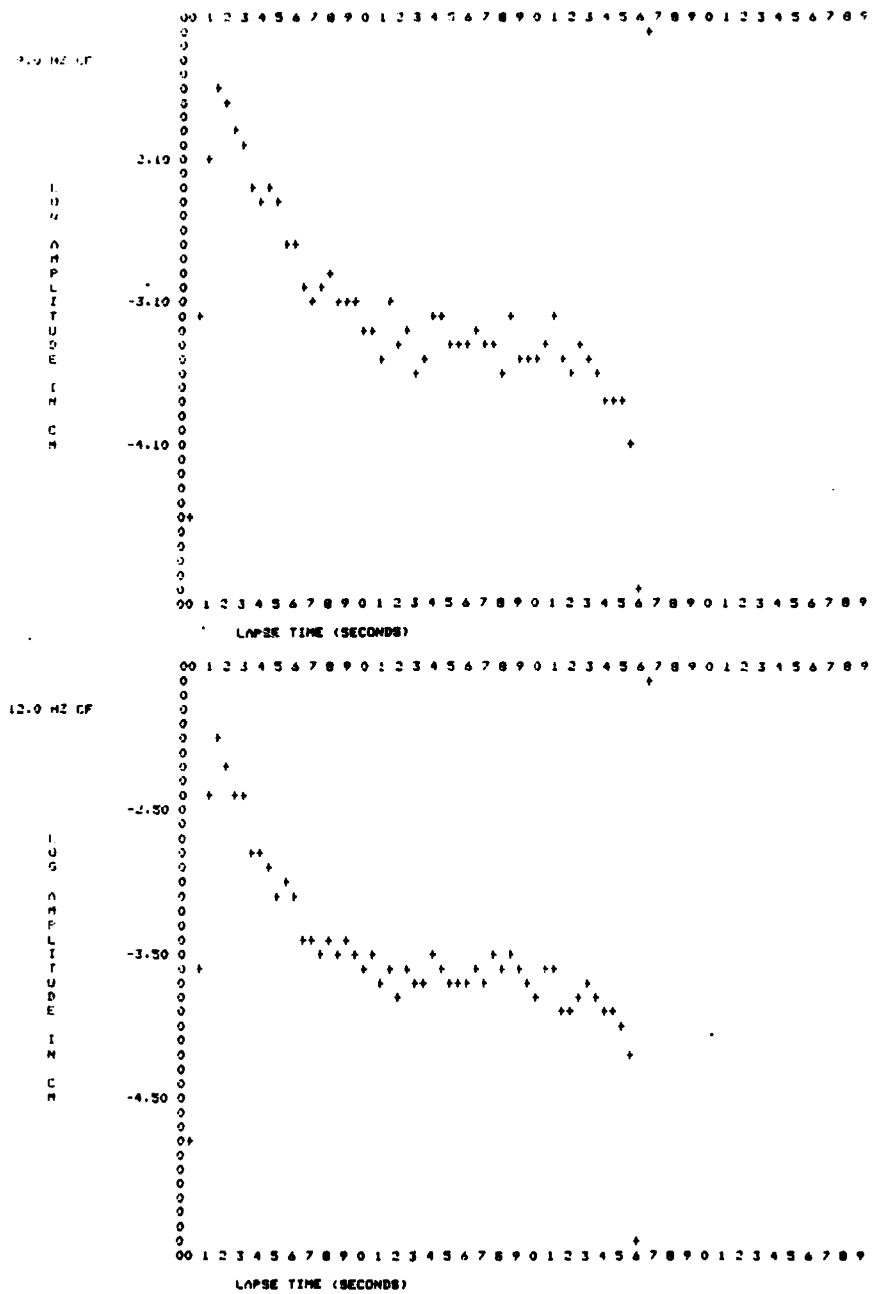

Figure 3. d.(top) e.(bottom)

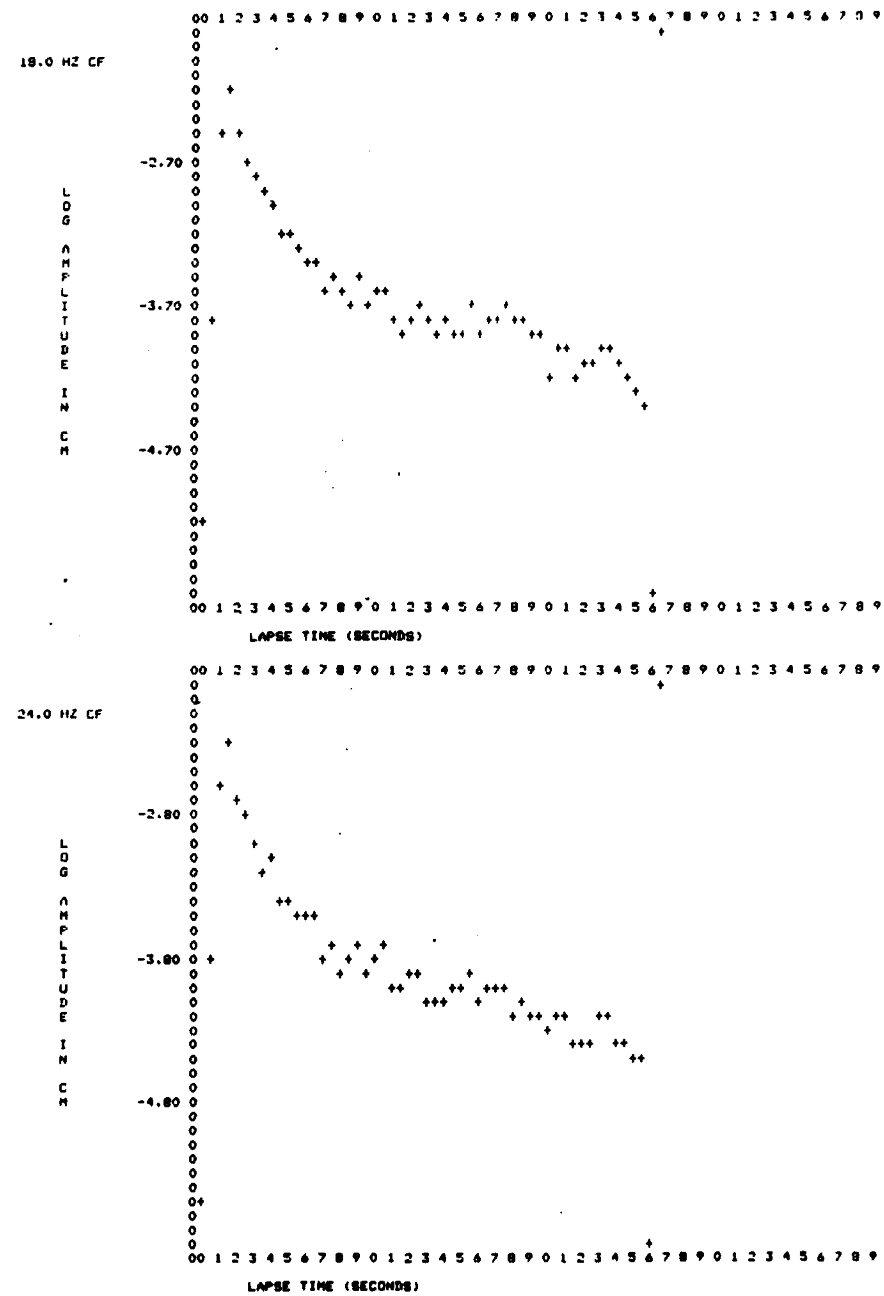

Figure 3 . f.(top) g.(bottom)

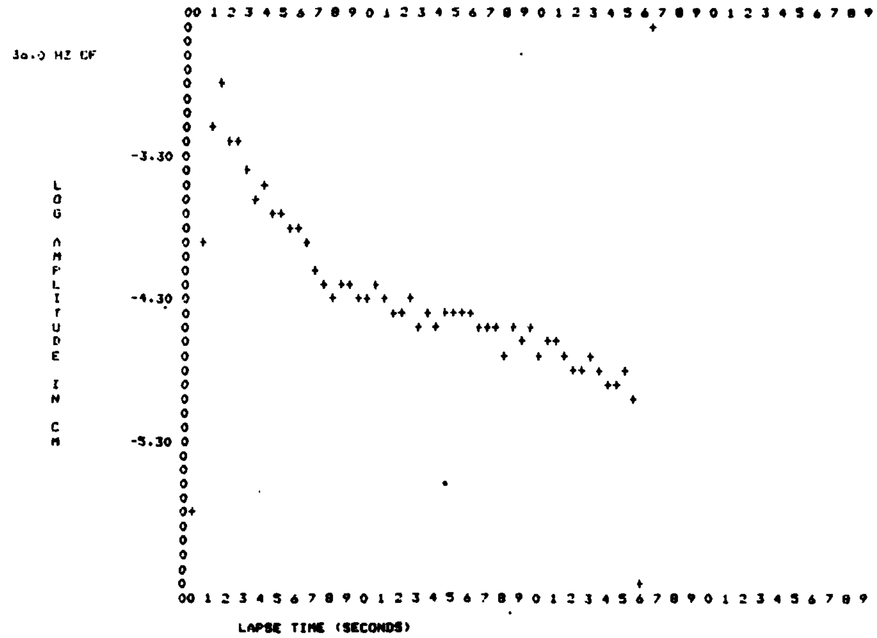

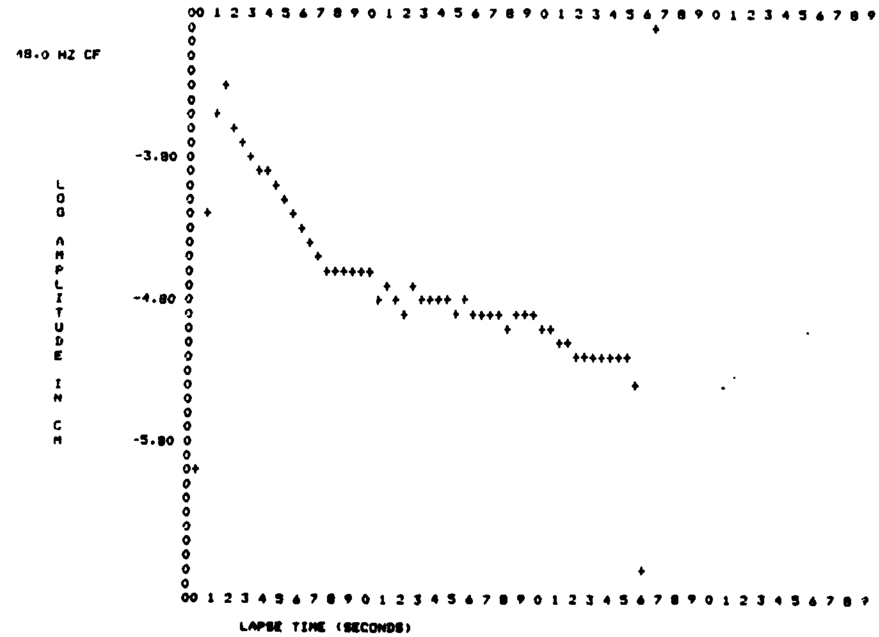

Figure 3. h.(top) i.(bottom)

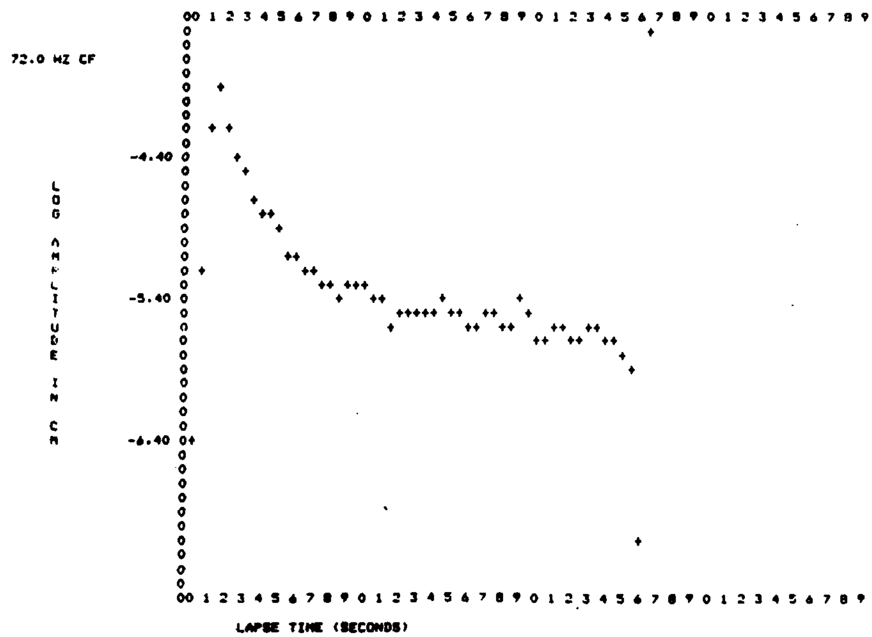

Figure 3. j.

The next step is to fit the model equation for $\log[A(f|t)]$ to the backscatter portion of the $\log[A(f|t)]$ plots for an estimate of Q_T. The method of least squares is used and two fits are made corresponding to the two choices of m = 1.0 and m = 0.5. Standard deviations are also calculated for each fit. Attempts to fit the model taking *m* as an independent variable produced erratic results as has been reported in the literature (Aki and Chouet, 1975).

The backscatter portion of the filtered data is determined as follows. Energy arriving after $\sqrt{2}$ times the primary S-wave travel time is backscatter in the sense that the scattering angle is greater than 90 degrees. However, because of the 1.28 second window and 0.5 second steps used for averaging only arrivals 1.0 second later than this are entirely backscatter.

On some records the dynamic range of the recording instrument has been exceeded for the early coda. The saturated portion of the coda is not considered in the analysis. Also excluded are the last three points of the filter output as they are distorted by artificial extension of the end of the trace necessary in filtering.

Another consideration is noise. The background noise level is assumed constant and taken equal to the peak noise level recorded prior to the P-wave arrival. If no noise is recorded here it is assumed to be + or - 0.5 times one unit of digitization. The noise level is converted to ground displacement amplitude. A reference, five times (14db above) this noise level, is taken as the minimum acceptable signal level. Portions of the coda for which the average signal amplitude falls below this reference are not considered in the fits.

Finally, from the longest records it is evident that Q_T changes with time causing the Q_T value obtained to depend on the portion of coda fit. This can be seen on the sample record in Figure 3. This time dependence of Q_T was also observed by Rautian and Khalturin (1978) who suggest variations of Q with depth and temporal variations of the geometric spreading factor as possible causes. The variation in spreading factor could result from a change in the type of waves being recorded as a function of time (e.g., surface to body waves as time increases). Another possibility is that of a significant deterministic influence on the energy arriving at the receiver. Long and Wilson (1982) have noticed resonance peaks in the power spectra of the Monticello records. The frequencies at which these occur are in congruence with conceivably supportable resonances in the Monticello reservoir. This can be regarded as an example of multiple scattering, which tends to raise the value of Q because energy previously scattered out of the coda is scattered back in, reducing the rate of decay. Indeed, in the limit of strong scattering, there is no contribution to Q from scattering (Dainty and Toksöz, 1977). Because of the observed temporal dependence of Q_T, fits are made to different portions of the coda where possible.

Results

Plots of the average over all stations and events of $\log[Q_T]$ versus log[frequency] are constructed and appear as Figure 4. Because a temporal dependence of Q_T was observed, three plots are made for each area and m value. They are from the beginning of backscatter to: I, five seconds beyond; II between five and nine seconds beyond; III,

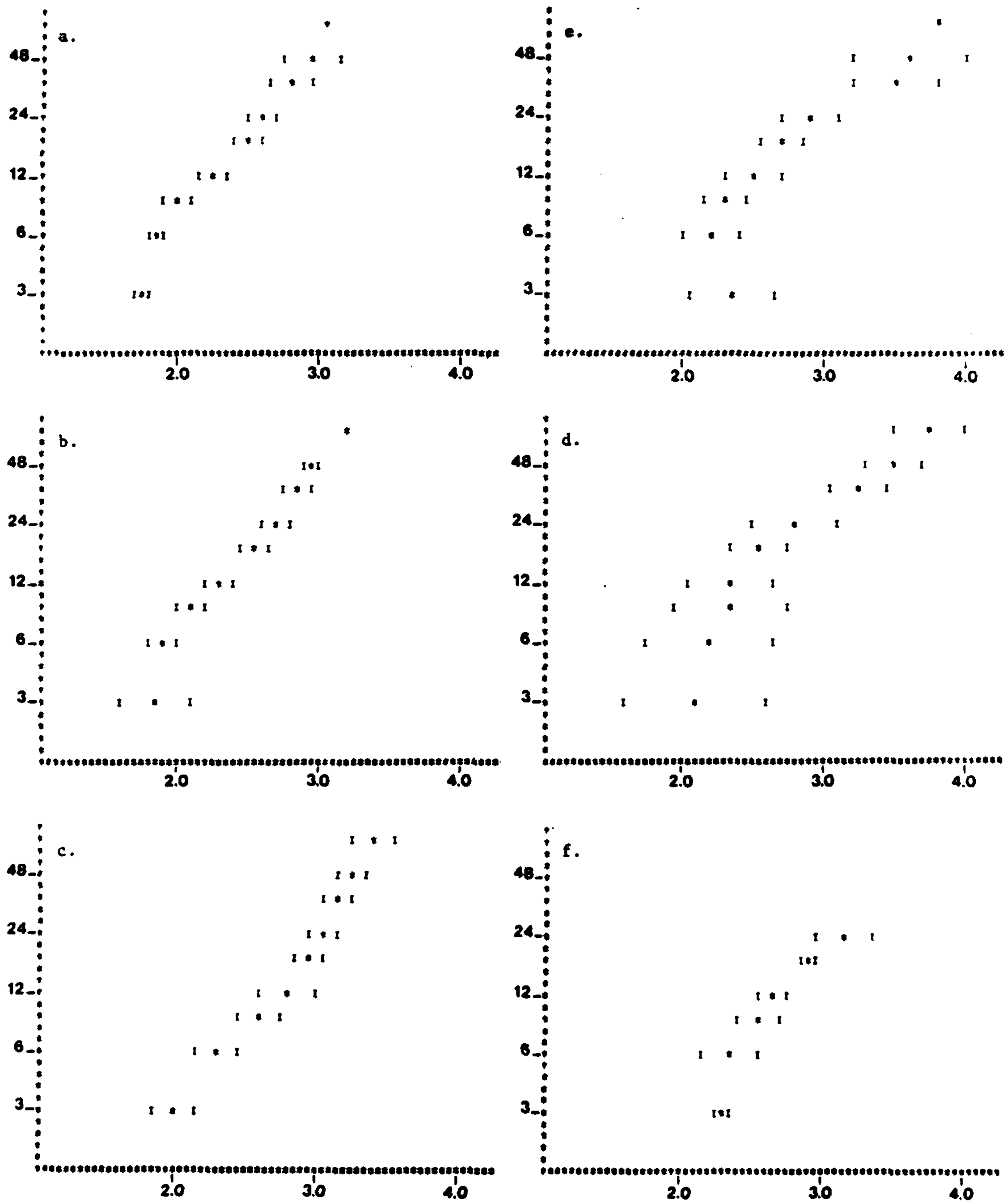

Figure 4a-f. Average log(Qtotal) versus Frequency, m=0.5. The vertical axes are frequency and the horizontal axes are log(Qtotal)
a, b, and c are for $t<5$, $5<t<9$, $9<t$ respectively at Monticello.
d, e, and f are for $t<5$, $5<t<9$, $9<t$ respectively at Mammoth.

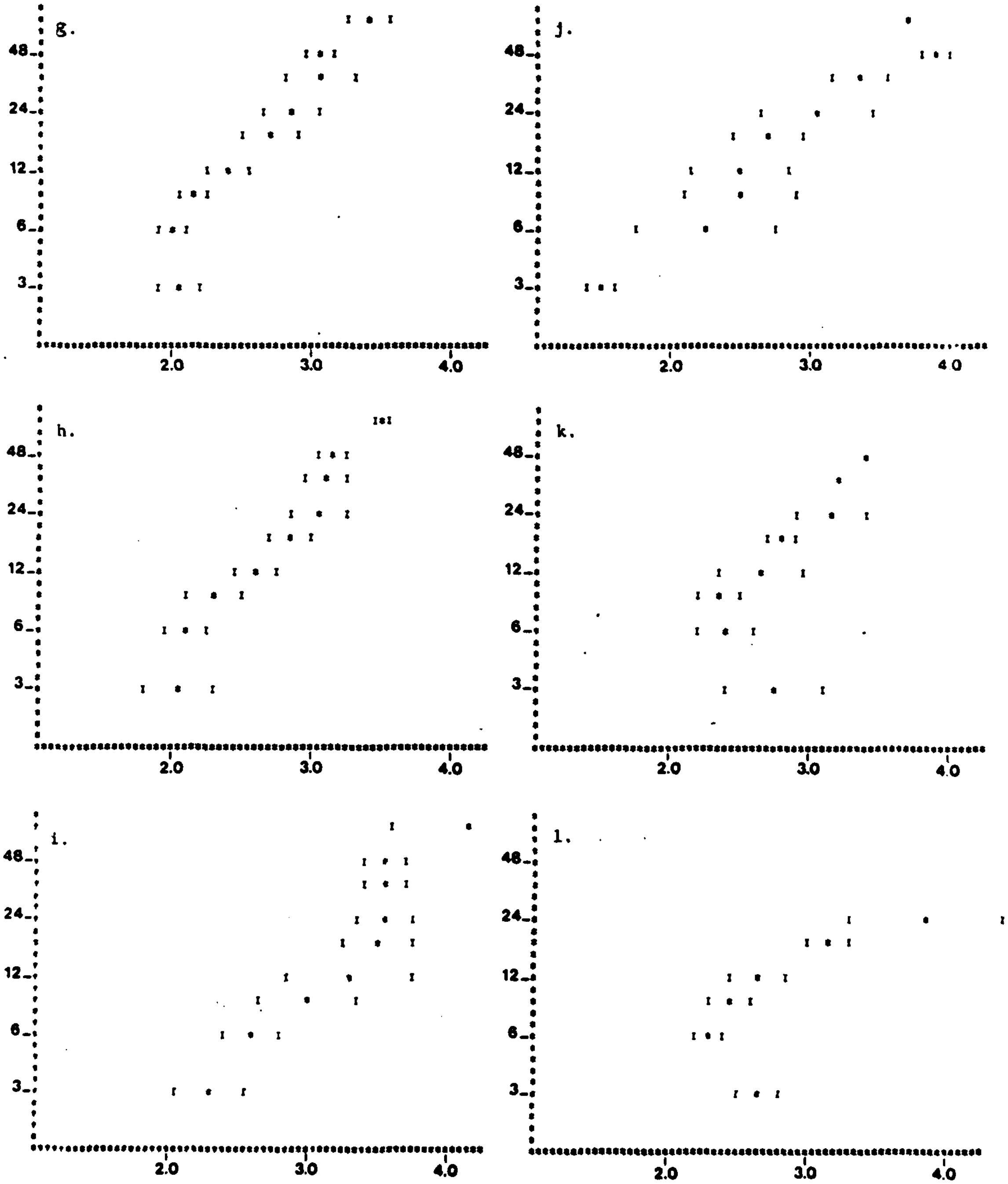

Figure 4g-1. Average log(Qtotal) versus Frequency, m=1.0. The vertical axes are frequency and the horizontal axes are log(Qtotal)
a, b, and c are for t< 5, 5<t< 9, 9<t respectively at Monticello.
d, e, and f are for t< 5, 5<t<9, 9<t respectively at Mammoth.

more than nine seconds beyond. These times were chosen arbitrarily within the limits of the data. As the plots are roughly linear, best fits of the equation $Q_T = af^b$ are made to each of these to determine the values of a and b. This approach is common in the literature. The a and b values obtained are presented in Table 3.

The frequency dependence of Q_T may be used to estimate Q_i and g if some assumptions are made about their frequency dependence. For the single backscatter model applied here the density of scatterers ρ is assumed constant. The backscatter cross section σ_b will be a constant for geometric (high frequency) scatter. The result is a constant g for geometric scatter with the single backscatter model. It is usually assumed that Q_i is independent of frequency in agreement with most laboratory measurements of Q_i (Knopoff, 1964). With these assumptions a least squares fit of $1/Q_T = 1/Q_i + gB/2\pi f$ is made to the Q_T versus frequency data to estimate g and Q_i (Dainty, 1981). Negative values of Q_i occur when the least square fit results in a $gB/2\pi f$ which is greater than $1/Q_T$. As Q_i increases with increasing $gB/2\pi f$ a negative Q_i result is indicative of a very high Q_i value. These results are shown in Table 4.

A second estimate of g is obtained as follows. From the least squares fit of log[A(f t)] estimates of Q_T and the source factor have been obtained. The filter output at the primary S-wave travel time at a given frequency is a component of the source factor C. This allows a second estimate of g from the primary S-wave spectra and the source factor $C = \log(s\Delta f)$.

Taking a result from the theory section

Table 3. Best Fit a and b Values. $Q_T = af^b$ at Monticello and Mammoth. m = 0.5 and m = 1.0 correspond to cylindrical and spherical spreading respectively.

	Monticello			Mammoth		
	a	b	freq	a	b	freq
m = 0.5						
I	6.3	1.2	6-48	1.5	1.8	3-24
I				6.2	0.6	12-72
II	9.7	1.1	3-72	4.1	1.6	6-72
III	31.8	1.0	3-72	16.6	1.3	6-24
m = 1.0						
I	9.2	1.2	6-72	9.0	1.4	3-36
II	11.0	1.2	6-72	20.0	1.2	6-48
III	29.6	1.5	3-24	7.6	1.7	6-24
III	2750	0	18-48			

Table 4. Log(g) Values From Fitting Equation (5).

	Monticello			Mammoth		
	log g	Q_i	freq	log g	Q_i	freq
<u>m = 0.5</u>						
I	-0.92	940	3-72	-1.28	1050	3-72
II	-1.00	900	3-72	-1.46	860	3-72
III	-1.19	*	3-72	-1.49	1050	3-24
<u>m = 1.0</u>						
I	-0.70	*	3-72	-1.17	1000	3-72
II	-1.92	610	3-72	-1.17	2960	3-48
III	-1.49	*	3-72	-1.82	580	3-24

* indicates Q_i approaching infinity.

$$s = \left|\phi(f|r_o)\right|^2 4m\pi r_o^{2m} (B/2)^{1-2m} g . \quad (11)$$

Also, the average amplitude, $\left|\phi(f|r)\right|$, of waves incident at a scatterer at distance r is

$$\left|\phi(f|r)\right| = \left|\phi(f|r_o)\right| (r/r_o)^{-m} \exp(-\pi f r/BQ_T) . \quad (12)$$

It is important to note that $\left|\phi(f|r)\right|$ is also the average spectral amplitude of the direct S-wave where r is the source receiver distance. This is estimated from a linear interpolation of the spectral amplitudes measured in the two windows closest to the S arrival time. The interpolation is necessary as the window is generally not centered on the S arrival. Solving equation (12) for the source spectrum at r_o, $\left|\phi(f|r_o)\right|$, and substituting in (11) a solution for log(g) is obtained.

$$\log(g) = 2C - \log[4m\pi(B/2)^{1-2m} \left|\phi(f|r)\right|^2 r^{2m} \exp(2\pi f t/Q_T)\Delta f] . \quad (13)$$

Estimates of average log(g) are obtained using this equation for m = 0.5 and or m = 1 and are tabulated in Table 5.

Discussion

The $\log(Q_T)$ versus log(frequency) curves of Figure 4 show Q_T to be roughly the same for similar fits at Mammoth and Monticello. Though it is generally agreed that Q_T is higher in the eastern U.S. the results here may be explained by the short lapse times of the codas used to estimate Q_T. These lapse times are much shorter than are usually reported in the literature for Q_T from coda estimates.

Table 5. Log(g) as Estimated from the S-wave Spectrum and Coda Source Function.

	Monticello		Mammoth	
	log g	freq	log g	freq
m = 0.5				
I	-2.50	3-72	-1.90	3-72
II	-2.53	3-72	-1.78	3-72
III	-3.27	3-72	-2.36	3-24
m = 1.0				
I	-3.03	3-72	-2.46	3-72
II	-2.96	3-72	-2.26	3-48
III	-3.50	3-72	-2.77	3-24

This implies that the results here represent the near surface Q_T and that it is approximately the same for both regions.

The results presented in Table 3 are the a and b values obtained by best fit of $Q_T = af^b$ to the log[Q_T] versus log[frequency] curves of Figure 5. The values of b in Table 3 range from 0.6 to 1.8, with an average of 1.3. The usual value of b reported in the literature is around 0.5 (0.6, Fedotov and Boldyrev, 1969; 0.5, Rautian and Khalturin, 1978; 0.5, Tsujiura, 1978; 0.6, Aki, 1980). However, the higher values obtained here are not unique. Rovelli (1982) has reported a b value of 1.1 for Friuli, Italy. This value was determined by coda analysis. Aki suggests that the b value, 0.8, which he determined for northeast Kanto, Japan, is the result of increased scattering by a higher density of scatterers associated with the higher level of tectonic activity in this part of the region. Aki and Chouet (1975) report on Q versus frequency at Stone Canyon, California. A b value of 0.9 is obtained by best fit of $Q_T = af^b$ to the reported results. Stone Canyon, Mammoth Lakes, and Friuli are all highly active regions.

The b value results at Monticello may be considered anomalous for this region of relative tectonic stability. However, in addition to including the reservoirs as a substantial part of the region sampled the codas and hypocentral distances at Monticello are much shorter than are usually reported in the literature for other studies. Consequently the near surface scatterers are favored in sampling. Andrews (1982) has suggested that near surface scattering is the dominant scattering effect for the similar situation at Mammoth Lakes.

Table 4 gives the results of fitting equation (5) to the values of Q_T as a function of frequency. Q_i and g are considered constants with frequency in making this fit. In (5), the two terms on the right hand side will be equal for a frequency F given by

$$F = gBQ_i/(2\pi) \tag{14}$$

Table 6 gives the values of F found using the results presented in Table 4. For frequencies less than F, scattering dominates the attenuation, while for frequencies greater than F, inelastic attenuation will dominate. From Table 6, scattering dominates attenuation over most of the frequency range in most cases, especially at Monticello. From (5), if scattering dominates then Q_T should be proportional to frequency, in approximate agreement with the results presented in Table 3. The proportionality of Q_T with frequency is also seen in Figure 4.

There is, however, another issue raised by Table 6. Dainty and Toksoz (1981) propose that if the frequency $f < F$, multiple scattering is a possibility. Obviously this situation holds for most of the codas considered here, from Table 6. Dainty and Toksoz point out that this seems to be true for many cases cited in the literature. However, Dainty and Toksoz's condition is only a necessary, not a sufficient, condition for multiple scattering. Since it will take some time after the origin time for multiple scattering to become important, a condition from Sato (1977) that multiple scattering will become important for times $t > T$, where $T = 1/(gB)$, is appropriate; if $f < F$ and $t > T$, strong scattering is probably occurring. T is also

Table 6. $F = gBQ_i/(2\pi)$, $T = 1/(gB)$. * is F tending to infinity.

	Monticello			Mammoth		
	F (Hz)	T (sec)	Freq. Range (Hz)	F (Hz)	T (sec)	Freq. Range (Hz)
m = 0.5						
I	60	2.4	3-72	30	5.4	3-72
II	50	2.9	3-72	15	8	3-72
III	*	4.4	3-72	20	9	3-24
m = 1.0						
I	*	1.4	3-72	40	4.2	3-72
II	4	24	3-72	100	4.2	3-48
III	*	9	3-72	5	19	3-24

given in Table 6, and in general indicates that multiple scattering might be occurring in some of the codas, remembering that I indicates $t \leq 5$ sec; II, $t \leq 9$ sec; III, $t > 9$ sec; but in practice t is less 30 sec for all codas in III. More generally, both F and T in Table 6 are of the same order of magnitude as the frequencies and times considered in this study, suggesting that the situation may be transitional between weak and strong scattering. A similar conclusion was reached by Dainty and Toksöz (1981). Theoretical formulations to handle this problem (e.g., Gao et al., 1983) do not appear to conserve energy and do not appear to agree with the strong scattering diffusion formalism of Dainty and Toksöz (1977).

The log[g] values obtained from the coda source spectrum are presented in Table 5. In general they are about an order of magnitude to two orders of magnitude smaller than the log[g] values obtained from Dainty's equation. Andrews (1982) has found the source spectral amplitude from the coda to be ten times larger than the spectral amplitude measured from the S-wave. As the value of g here is proportional to the quotient (coda source spectrum/S wave source spectrum), a small g value means our results do not agree with those of Andrews'. However, they are in agreement with the theoretical results reported in the second part of this report.

Throughout this report, the question of whether the scattering is two-dimensional ($m = 0.5$, cylindrical spreading, surface waves) or three-dimensional ($m = 1.0$, spherical spreading, body waves) has been left open. As discussed in the section on Analysis, it was not possible to determine the correct value of m from the data. Aki

(1980) has suggested on various grounds that the three-dimensional case is probably appropriate, but he dealt with much longer codas. Most of the more important results presented here seem to hold for both cases. It must be conceded, however, that the change in coda decay as time increases could be due to a change in Q_T reflecting the change from surface waves to body waves.

Bibliography

Aki, K. (1969). Analysis of the seismic coda of local earthquakes as scattered waves, J. Geophys. Res., 74, 615-631.

Aki, K. (1980). Scattering and attenuation of shear-waves in the lithosphere, J. Geophys. Res., 85, 6496-6504.

Aki, K., and Chouet, B. (1975). Origin of coda waves: source, attenuation, and scattering effects, J. Geophys. Res., 80, 3322-3342.

Andrews, D. J. (1982). Shear wave and coda attenuation of two aftershocks at Mammoth Lakes, California (abstract), EOS, 63, 1029.

Archuleta, R. J., Cranswick, E., Mueller, C., and Spudich, P. (1982). Source parameters of the 1980 Mammoth Lakes, California, earthquake sequence, J. Geophys. Res., 87, 4595-4607.

Chernov, L. A. (1960). Wave Propagation in a Random Medium, McGraw-Hill, New York.

Dainty, A. M. (1981). A scattering model to explain seismic Q observations in the lithosphere between 1 and 30 Hz, Geophys. Res. Letters, 8, 1126-1128.

Dainty, A. M., and Toksöz, M. N. (1977). Elastic wave propagation in a highly scattering medium--a diffusion approach, J. Geophys., 43, 375-388.

Dainty, A. M., and Toksöz, M. N. (1981). Seismic codas on the Earth and the Moon: a comparison, Phys. Earth Planet. Interiors, 26, 250-260.

Fedotov, S. A., and Bolydrev, S. A. (1969). Frequency dependence of the body waves absorption in the crust and upper mantle of the Kuril Islands chain, Izv. Akad. Nauk. SSSR, 9, 17-33.

Fletcher, J. B. (1982). A comparison between the tectonic stress measured in situ and stress parameters from induced seismicity at Monticello Reservoir, South Carolina, J. Geophys. Res., 87, 6031-6944.

Galkin, I. N., Nikolayev, A. V., and Starshinova, YE. A. (1970). Fluctuations of wave characteristics and small-scale inhomogeneities of the Earths crust, Izv. Earth Physics, 11, 41-48.

Gao, L. S., Lee, L. C., Biswas, N. N., and Aki, K. (1983). Comparison of the effects between single and multiple scattering on coda waves for local earthquakes, Bull. Seismol. Soc. Amer., 73, 377-389.

Klein, F. W. (1978). Hypocenter location program HYPOINVERSE, 1: Users guide to versions 1,2,3,and 4, U.S. Geol. Surv. Open File Rept. 78-694.

Knopoff, L. (1964). Q, Rev. Geophys., 2, 625-660.

Knopoff, L., and Hudson, J. A. (1967). Frequency dependence of scattered elastic waves, J. Acoust. Soc. Am., 42, 18-20.

Long, L. T., and Wilson, J. (1982). Personal communication.

Rautian, T. G., and Khalturin, V. I. (1978). The use of the coda for determination of the earthquake source spectrum, Bull. Seismol. Soc. Amer., 68, 923-948.

Rovelli, A. (1982). On the frequency dependence of Q in Fruili from short period digital records, Bull. Seismol. Soc. Amer., 72, 2369-2372.

Sato, H. (1977). Energy propagation including scattering effects single isotropic scattering approximation, J. Phys. Earth, 27-41.

Secor, Jr., D. T., Peck, L. S., Pitcher, D. M., Prowell, D. C., Simpson, D. H., Smith, W. A., and Snoke, A. W. (1982). Geology of the area of induced seismic activity at Monticello Reservoir, South Carolina, J. Geophys. Res., 87, 6945-6957.

Spudich, P., Cranswick, E., Fletcher, J., Harp, E., Mueller, C., Navarro, R., Sarmiento, J., Vinton, J., and Warrick, J. (1982). Acquisition of digital seismograms during the Mammoth Lakes, California, earthquake sequence of May-June 1980, U.S. Geol. Surv. Open-File Rept. 81-38.

Talwani, P., and Hutchenson, K. D. (1982). Induced seismicity and earthquake prediction studies in South Carolina, U.S. Geol. Surv. Final Technical Report, contract no. 14-08-0001-19252.

Tsujiura, M. (1978). Spectral analysis of the coda waves from local earthquakes, Bull. Earthquake Res. Inst., Tokyo Univ., 53, 1-48.

Wallace, T., Given, J., and Kanamori, H. (1982). A discrepancy between long- and short-period mechanisms of earthquakes near the Long Valley Caldera, Geophys. Res. Lett., 9, 1131-1134.

Wu, Ru-Shan (1982). Attenuation of short period seismic waves due to scattering, Geophys. Res. Lett., 9, 9-12.

Zoback, M. D., and Hickman, S. (1982). In situ study of the physical mechanisms controlling induced seismicity at Monticello Reservoir, S.C., J. Geophys. Res., 87, 6959-6974.

APPENDIX 2

JOURNAL OF GEOPHYSICAL RESEARCH, VOL. 89, NO. B5, PAGES 3172–3176, MAY 10, 1984

High-Frequency Acoustic Backscattering and Seismic Attenuation

ANTON M. DAINTY

School of Geophysical Sciences, Georgia Institute of Technology

An expression for the backscattered intensity of acoustic waves singly scattered from a region containing fluctuations of the acoustic velocity has been derived for high frequencies by expanding the autocorrelation of the slowness fluctuations in a Taylor series about zero lag. The resulting expression indicates that the backscattered intensity is independent of frequency and directly proportional to the first derivative of the autocorrelation at zero lag; the next higher term is proportional to the reciprocal of the square of the frequency and directly proportional to the third derivative of the autocorrelation at zero lag. Contributions from terms of the Taylor series involving even numbered derivatives of the autocorrelation are zero. Since for the autocorrelation of a smooth function only the even numbered derivatives are nonzero at zero lag, this result demonstrates that backscattering at high frequencies can only occur from discontinuities of velocity or its derivatives as opposed to fluctuations in which the velocities are smooth. If the backscattered intensity is independent of frequency, the contribution of backscattering to the attenuation parameter Q is proportional to frequency. Such behavior may have been observed for seismic waves of frequencies greater than 1 Hz, suggesting that scattering from discontinuities is an important part of the attenuation of such waves.

INTRODUCTION

The phenomenon of scattering of seismic waves has attracted increasing attention in recent years. Backscattering of seismic waves has been used to explain terrestrial codas [*Aki and Chouet*, 1975; *Dainty and Toksoz*, 1981] and part or all of the attenuation suffered by seismic waves at frequencies of 1 Hz and greater [*Aki*, 1980; *Dainty*, 1981; *Kikuchi*, 1981; *Wu*, 1982]. To analyze observed data on attenuation, coda amplitudes and other manifestations of scattering, a model of the earth as a scattering medium is required together with a theory to derive quantitative results from this model. Two general types of model have been used. One is the "randomly distributed specific scatterers" model. This model assumes scatterers of a specific type, for example, spheres, randomly distributed throughout an otherwise homogeneous region. Examples of this type of model are the sphere model of *Dainty* [1981], used to explain the frequency dependence of the attenuation parameter Q at frequencies above 1 Hz, and the crack model of *Kikuchi* [1981], also used to analyze Q. A second type of model is the "random medium" model, in which the earth is considered to have average properties that do not vary from place to place but with random fluctuations of the material properties. Examples are the use of an acoustic random medium by *Aki* [1980] and *Wu* [1982] to analyze Q above 1 Hz.

In this paper I shall examine the acoustic random medium model using the results of *Chernov* [1960] in the limit of high-frequency backscattering. This problem was chosen because investigators using this model have generally concluded that this is the practical case in the earth for frequencies of 1 Hz and higher [*Aki*, 1980; *Dainty*, 1981; *Sato*, 1982*b*; *Wu*, 1982]. By analyzing the high-frequency limit, insight may be gained as to what type of information about the medium may be deduced from high-frequency data. An additional benefit is an understanding of the relationship between the two types of models that have been used to examine this problem.

Paper number 4B0124.
0148-0227/84/004B-0124$05.00

RANDOM MEDIUM MODELS

The simplest type of random medium used in seismology is the acoustic random medium discussed by *Chernov* [1960] (a summary of some useful results is given by *Aki and Richards* [1980]). The medium is considered to have fluctuations of velocity and density about mean values; for simplicity I will consider only the velocity fluctuations. Let the acoustic velocity C be given by

$$C = C_0[1 - \mu(\mathbf{x})] \tag{1}$$

where C_0 is a constant and $\mu(\mathbf{x})$, the slowness perturbation, is a random function of position $\mathbf{x}$ and has an average value of zero. The autocorrelation $N(\mathbf{r})$ of the slowness perturbation μ is then

$$N(\mathbf{r}) = \langle \mu(\mathbf{x})\mu(\mathbf{x} + \mathbf{r})\rangle / \langle \mu^2 \rangle \tag{2}$$

The vector $\mathbf{r}$ is the lag, and the angle brackets indicate averaging over all $\mathbf{x}$. If the fluctuation is isotropic, then

$$N(\mathbf{r}) = N(r) \tag{3}$$

that is, the autocorrelation depends only on the magnitude of the lag and not its direction.

Chernov [1960] finds the amplitude of singly (weakly) scattered waves for the case of a plane wave traveling through an acoustic medium of velocity C_0 without velocity fluctuations, except for a volume V containing velocity fluctuations as described above. If the incident (pressure) wave is given by

$$p_i = A \cdot \exp\,[2\pi f i(t - x/C_0)] \tag{4}$$

where f is the frequency, then the amplitude of the scattered wave at position $\mathbf{R}$ from the center of V in the limit of R large in comparison with the linear dimension of V is given by

$$|p_s|^2 = \frac{4\pi^2 V A^2 f^3 \langle \mu^2 \rangle}{C_0{}^3 R^2 \sin(\theta/2)} \cdot \int_0^\infty N(r) \cdot \sin\{[4\pi f r \cdot \sin(\theta/2)]/C_0\} \quad r\,dr \tag{5}$$

[*Chernov*, 1960, equation 45, p. 51]. The scattering angle θ is the angle between $\mathbf{R}$ and the direction of propagation; I shall define "backscattering" as the case $\theta > \pi/2$. Equation (5) was first derived, in a slightly different form, by *Pekeris* [1947].

This paper is concerned with the evaluation of (5) in the limit of large f and $\theta > \pi/2$.

Before proceeding, it should be noted that the acoustic medium described above is obviously too simple to describe the earth, which is an elastic medium presumably containing fluctuations of both elastic constants and density and through which two types of waves, compressional and shear, can propagate. *Knopoff and Hudson* [1967] have demonstrated that converted waves (scattered compressional waves from incident shear waves, and vice versa) are not important at high frequencies. *Haddon and Cleary* [1974] examined the problem of scattering from an inhomogeneous elastic medium; some of their (unpublished) results are discussed in the work of *Aki and Richards* [1980]. These results indicate that at least some of the formulas equivalent to equation (5) are of a similar form. Accordingly, (5) may be considered typical of integrals that appear in this type of problem.

EVALUATION OF THE BACKSCATTERED INTENSITY AT HIGH FREQUENCY

To evaluate (5), we need to find the integral

$$\int_0^\infty N(r)\cdot \sin\{[4\pi fr\cdot\sin(\theta/2)]/C_0\}\cdot r\,dr = F(\infty) - F(0) \tag{6}$$

where F is the indefinite integral. However, if there is a scale length a associated with the fluctuations, $N(r)$ will generally decline rapidly for r larger than a. Accordingly, I will assume that $F(\infty)\rightarrow 0$ in (6); this will certainly be true of $N(r)\rightarrow \exp[-r/a]$ for large r. Then

$$\int_0^\infty N(r)\cdot \sin\{[4\pi fr\cdot\sin(\theta/2)]/C_0\}\cdot r\,dr \cong -F(0) \tag{7}$$

To approximate $F(0)$ in the case of f large and $\theta > \pi/2$, note that for this case the sine term in (7) varies much more rapidly than $N(r)$, assuming N is a smooth function. Accordingly, I will expand $N(r)$ in a Taylor series near $r = 0$. First, however, define

$$u = [4\pi fr\cdot\sin(\theta/2)]/C_0 \tag{8}$$

$$K = [4\pi f\cdot\sin(\theta/2)]/C_0 \tag{9}$$

Then (7) becomes

$$\frac{1}{K^2}\int_0^\infty N\left(\frac{u}{K}\right)\cdot\sin(u)\cdot u\,du \cong -F(0) \tag{10}$$

Expand $N(u/K)$ as, remembering that $u/K = r$,

$$N\left(\frac{u}{K}\right) = N(0) + \frac{u}{K}\left(\frac{dN}{dr}\right)_{r=0} + \frac{1}{2}\left(\frac{u}{K}\right)^2\left(\frac{d^2N}{dr^2}\right)_{r=0} + \cdots \tag{11}$$

provided the derivatives at $r = 0$ exist and are finite. Then

$$F(u) \cong \frac{1}{K^2}\left[N(0)\int u\cdot\sin(u)\cdot du + \frac{1}{K}\left(\frac{dN}{dr}\right)_{r=0}\cdot\int u^2\sin(u)\cdot du + \frac{1}{2K^2}\left(\frac{d^2N}{dr^2}\right)_{r=0}\cdot\int u^3\sin(u)\cdot du + \cdots\right] \tag{12}$$

To evaluate (12), use the tabulated integrals [*Carmichael and Smith*, 1962]:

$$\int u\cdot\sin(u)\cdot du = \sin(u) - u\cdot\cos(u) \tag{13}$$

$$\int u^m\sin(u)\cdot du = -u^m\cos(u) + m\int u^{m-1}\cos(u)\cdot du \tag{14}$$

$$\int u^m\cos(u)\cdot du = u^m\sin(u) - m\int u^{m-1}\sin(u)\cdot du \tag{15}$$

$$\int u\cdot\cos(u)\cdot du = \cos(u) + u\cdot\sin(u) \tag{16}$$

Using (14) and (16),

$$\int u^2\sin(u)\cdot du = 2u\cdot\sin(u) + (2-u^2)\cos(u) \tag{17}$$

Using (13), (14), (15), and (16),

$$\int u^m\sin(u)\cdot du = \cos(u)\cdot\left[-u^m + \sum_{n=1}^{(m-1)/2}(-1)^{n+1}\cdot m(m-1)\cdots(m-2n+1)u^{m-2n}\right] + \sin(u)\left[mu^{m-1} + \sum_{n=1}^{(m-1)/2}(-1)^n\cdot m(m-1)\ldots(m-2n)u^{m-2n-1}\right] \tag{18}$$

(m odd)

$$\int u^m\sin(u)\cdot du = \cos(u)\left[-u^m + \sum_{n=1}^{m/2}(-1)^{n+1}\cdot m(m-1)\ldots(m-2n+1)u^{m-2n}\right] + \sin(u)\left[mu^{m-1} + \sum_{n=1}^{(m/2)-1}(-1)^n\cdot m(m-1)\ldots(m-2n)u^{m-2n-1}\right] \tag{19}$$

(m even)

From (13), (17), (18), and (19), as $u\rightarrow 0$,

$$\int u\cdot\sin(u)\cdot du\rightarrow 0 \tag{20}$$

$$\int u^2\sin(u)\cdot du\rightarrow 2 \tag{21}$$

$$\int u^m\sin(u)\cdot du\rightarrow 0 \qquad (m\text{ odd}) \tag{22}$$

$$\int u^m\sin(u)\cdot du\rightarrow(-1)^{m/2+1}m! \qquad (m\text{ even}) \tag{23}$$

Substituting in (12) and letting $u\rightarrow 0$,

$$F(0) = \sum_{n=1}^{\infty}\frac{1}{K^{2n+1}}(-1)^{n+1}\frac{(2n)!}{(2n-1)!}\left(\frac{d^{2n-1}N}{dr^{2n-1}}\right)_{r=0} \tag{24}$$

According to (24), under the conditions described the backscattered intensity depends only on the odd derivatives of N at $r = 0$ and not on the even derivatives. Since this is a high-frequency approximation, the first term in (24) will be the most important, that is,

$$F(0) \cong \frac{2}{K^3}\left(\frac{dN}{dr}\right)_{r=0} + O(1/K^5) \tag{25}$$

Substituting in (10) and (5),

$$|p_s|^2 = -\frac{VA^2\langle\mu^2\rangle}{8\pi R^2 \sin^4(\theta/2)}\left(\frac{dN}{dr}\right)_{r=0} + O(1/f^2) \quad (26)$$

This indicates that the backscattered intensity is independent of frequency, provided that the autocorrelation has a nonzero derivative at zero lag. Since the first derivative at zero lag must be negative ($N(r)$ has a maximum at $r=0$), $|p_s|^2$ will be positive.

To test (26), I will compare it to two specified cases of $N(r)$ for which explicit formulas for $|p_s|^2$ are available [*Chernov*, 1960]. If

$$N(r) = \exp(-r/a) \quad (27)$$

then

$$|p_s|^2 = \frac{32\pi^3 VA^2 f^4 a^3\langle\mu^2\rangle}{R^2[C_0^2 + 16\pi^2 f^2 a^2 \sin^2(\theta/2)]^2} \quad (28)$$

$$|p_s|^2 \rightarrow \frac{VA^2\langle\mu^2\rangle}{8\pi R^2 a \cdot \sin^4(\theta/2)} \qquad f\rightarrow\infty,\ \theta \geq \pi/2 \quad (29)$$

The approximate solution given by (26) reproduces this result.

Another case for which an exact solution is available is

$$N(r) = \exp(-r^2/a^2) \quad (30)$$

Then

$$|p_s|^2 = \frac{4\pi^{7/2} VA^2 f^4 a^3 \langle\mu^2\rangle}{R^2} \cdot \exp\{-[4\pi^2 f^2 a^2 \sin^2(\theta/2)]/C_0^2\} \quad (31)$$

$$|p_s|^2 \rightarrow 0 \qquad f\rightarrow\infty \qquad \theta \geq \pi/2) \quad (32)$$

Since $N(r)$ has no nonzero derivatives of odd order for $r=0$, this is also in accord with (26).

Discussion

The limit of validity of (26) can be obtained from (7), since we require that the sine terms in (7) vary much more rapidly than $N(r)$. If a is a scale length describing the range of r over which $N(r)$ varies appreciably, we must have

$$[4\pi f a \cdot \sin(\theta/2)]/C_0 \gg 2\pi \quad (33)$$

or

$$[2fa \cdot \sin(\theta/2)]/C_0 \gg 1 \quad (34)$$

Note that (34) requires that the scattering angle θ cannot be small; in fact,

$$\sin(\theta/2) \gg C_0/(2fa) \qquad \theta \geq 30^\circ \quad (35)$$

is necessary. Thus the approximation used here is not valid for forward scattering. It may, however, be valid for $\theta < \pi/2$ provided the restriction (35) is observed, together with a restriction discussed below requiring $\theta \geq 30^\circ$. Within these limits, the scattered intensity varies as $1/(\sin^4 \theta/2)$, indicating that "side scattering" ($\theta \sim \pi/2$) is about 4 times as strong as "backscattering" ($\theta \sim \pi$) in the strict sense.

There is, however, another consideration that must be applied to the forward scattering question. In forward scattering ($\theta \rightarrow 0$) the scattered wave merges with the original incident wave [*Chernov*, 1960; *Knopoff and Hudson*, 1967]. The theory used to derive (5) does not satisfactorily account for this [*Chernov*, 1960] and accordingly (26) should never be used for small θ, (35) notwithstanding. *Sato* [1982*a*], in fact, indicates that the merging of the scattered and incident wave is a significant effect for $\theta \leq 30^\circ$ (see (44) and (45), below), and thus I have added the restriction $\theta \geq 30^\circ$ to (35). It should also be noted, however, that if $(dN/dr)_{r=0} \neq 0$, (26) indicates that there is always backscattered energy, no matter how high the frequency of the incident wave. I shall examine the type of velocity fluctuation that gives rise to such a situation below.

An important application of the theory of backscattering is the interpretation of the frequency variation of Q for shear waves in the range 1–30 Hz [*Aki*, 1980; *Wu*, 1982]. Q, the quality factor, describes the attenuation of the amplitude A in (4) by

$$A(x) = A(0)\exp[-\pi f x/(QC_0)] \quad (36)$$

The total Q represents the effects of energy loss from the primary wave by the combined mechanisms of loss of seismic energy to heat (Q_i) and loss due to backscattering (Q_s) according to the relation [*Warren*, 1972]

$$1/Q = 1/Q_i + 1/Q_s \quad (37)$$

Wu [1982] derives an expression for Q_s, with the proper choice of V, as

$$1/Q_s = \frac{C_0 R^2}{2\pi f A^2 V}\int_0^{2\pi} d\phi \int_{\pi/2}^{\pi} d\theta\, |p_s|^2 \sin(\theta) \quad (38)$$

where ϕ is an azimuthal angle about the direction of propagation of the primary wave and the integral over scattering angle θ is taken over all backscattering angles.

Substituting for $|p_s|^2$ from (26) and performing the integral over ϕ, in the limit of high frequency,

$$1/Q_s = -\frac{C_0\langle\mu^2\rangle}{8\pi f}\left(\frac{dN}{dr}\right)_{r=0}\int_{\pi/2}^{\pi}\frac{\sin(\theta)\,d\theta}{\sin^4(\theta/2)} \quad (39)$$

This may be evaluated using the trigonometric identity

$$2\sin^2(\theta/2) = 1 - \cos(\theta) \quad (40)$$

as

$$1/Q_s = -\frac{C_0\langle\mu^2\rangle}{4\pi f}\left(\frac{dN}{dr}\right)_{r=0} \quad (41)$$

Comparing this with an expression from *Dainty* [1981],

$$1/Q_s = gC_0/(2\pi f) \quad (42)$$

then

$$g = -\frac{\langle\mu^2\rangle}{2}\left(\frac{dN}{dr}\right)_{r=0} \quad (43)$$

This indicates that g, the turbidity, is independent of frequency and depends on the product of the mean square slowness fluctuation and the derivative of the autocorrelation of the slowness fluctuation. The lack of dependence of g on frequency is the same result obtained by *Dainty* [1981] for a set of randomly distributed spheres in geometric scatter; thus we may say that the approximation explored in this paper is the analog of geometric scattering from obstacles. Indeed, observationally we cannot distinguish between these cases, nor can we distinguish between different autocorrelation functions $N(r)$ except insofar as their derivatives at $r=0$ differ. The lack of dependence of g on frequency may be experimentally observed for seismic waves above 1 Hz [*Dainty*, 1981].

In (38) the integral over the scattering angle was taken over all backscattered angles. *Sato* [1982*a*] has used a different approach (the mean wave method) from that used by *Chernov* [1960] and *Wu* [1982]. His work suggests that instead of (38),

$$1/Q_s = \frac{C_0R^2}{2\pi f A^2 V}\int_0^{2\pi} d\phi \left[\int_{\theta_c}^{\pi} d\theta\, |p_s|^2 \sin(\theta) + \int_0^{\theta_c} d\theta\, |p_s|^2 \sin^4(\theta/2)\sin(\theta)\right] \quad (44)$$

$$\sin(\theta_c/2) = 1/4 \qquad \theta_c \cong 30° \quad (45)$$

Comparing (44) and (38), *Sato* [1982*a*] indicates that all energy scattered at angles greater than θ_c should be considered lost from the primary wave (the first integral in the brackets) and a fraction of the more forward scattered energy should also be excluded (the second integral). *Wu* [1982] excluded only the backscattered energy. To evaluate (44), I shall use (26); while (26) is not valid near $\theta = 0$, the presence of the weighting factor $[\sin^4(\theta/2)\sin(\theta)]$ in (44) ensures that the integral is small in this region. Then

$$1/Q_s \cong -\frac{7}{2\pi}\frac{C_0\langle\mu^2\rangle}{f}\left(\frac{dN}{dr}\right)_{r=0} \quad (46)$$

from (42) this gives

$$g \cong -7\langle\mu^2\rangle\left(\frac{dN}{dr}\right)_{r=0} \quad (47)$$

The value in (47) is larger than that in (43) because a greater part of the scattered energy was considered lost from the primary wave.

The results in (43) and/or (47) may be compared with another parameter, the backscattering turbidity

$$g_\pi = \frac{R^2}{AV}|p_s(\pi)|^2 \quad (48)$$

$$g_\pi = -\frac{\langle\mu^2\rangle}{8\pi}\left(\frac{dN}{dr}\right)_{r=0} \quad (49)$$

This parameter controls the amplitude level of coda waves relative to the direct wave, after correction for geometrical spreading and attenuation [*Aki and Chouet*, 1975]. *Aki* [1980] suggested that $g_\pi \sim g$; *Sato* [1982*b*] presented a more detailed calculation. According to the formulas presented here,

$$g_\pi/g = 1/(4\pi) \cong 10\% \quad (50)$$

if expression (43) is used for g,

$$g_\pi/g \cong 1/(56\pi) \cong 1\% \quad (51)$$

if (47) is used for g.

A final, important question has to do with the nature of the slowness fluctuation $\mu(x)$ that will lead to an autocorrelation $N(r)$ that has a nonzero first derivative at $r = 0$. *Chernov* [1960] asserts that the first derivative of $N(r)$ must tend to zero for $r \to 0$ if $\mu(x)$ is continuous, although a proof is only given for the one-dimensional case. This is a special case of a result due to *Taylor* [1920], who proved (for the one-dimensional case) that the autocorrelation of a continuous function has only even-ordered derivatives that are nonzero at zero lag. *Pekeris* [1942] comments further on Taylor's result. However, K. Aki (personal communication, 1983) has pointed out that the (one-dimensional) function

$$\mu(x) = \int_{-\infty}^{\infty} w(\tau)h(x-\tau)\,d\tau \quad (52)$$

$$h(x) = \exp[-x/a] \qquad x > 0$$
$$= 0 \qquad x < 0 \quad (53)$$

has the autocorrelation given by (27) if $w(x)$ is any function with a power spectrum that is constant with frequency. If $w(x)$ is chosen to be "white noise," considered to be a set of impulses infinitely closely spaced, it appears that (52) may be continuous, even though it has an autocorrelation which has a nonzero first derivative at zero lag. However, the first derivative of (52) is

$$\mu'(x) = \int_{-\infty}^{\infty} w(\tau)h'(x-\tau)\,d\tau = \int_{-\infty}^{\infty} w(\tau)[\delta(x-\tau) - (1/a)h(x-\tau)]\,d\tau = w(x) - (1/a)\mu(x) \quad (54)$$

This is a discontinuous function, since $w(x)$ is discontinuous. Thus the function $\mu(x)$ is "continuous" but is not "smooth." This property of $\mu(x)$ is perhaps the reason that *Taylor*'s [1920] and *Chernov*'s [1960] proofs fail. The lack of smoothness may explain why the results obtained here are equivalent to geometrical scattering from obstacles, since in this case scattering at high frequencies is controlled by the discontinuity which is the boundary of the obstacle. Furthermore, this discontinuity will scatter waves of any frequency.

As an additional limitation on the theory presented here, I note that there is a class of autocorrelation functions, the Von Karman function [*Wu*, 1982; *personal communication*, 1983] that have infinite slopes at $r = 0$ for certain values of their parameters. The Von Karman function is given by

$$N(r) = \frac{1}{2^{m-1}\Gamma(m)}\left(\frac{r}{a}\right)^m K_m\left(\frac{r}{a}\right) \quad (55)$$

where $\Gamma(m)$ is the gamma function and K_m is the modified Bessel function. For $m < 1/2$, $(dN/dr)_{r=0} \to \infty$. Obviously, the theory presented here cannot apply to this case, since we may not write (11). For $m = 1/2$, (55) becomes (27), and for $m > 1/2$, $(dN/dr)_{r=0} \to 0$.

Acknowledgments. K. Aki, J.-C. Mareschal, W. Menke, Ru-Shan Wu, and an anonymous reviewer made suggestions that enhanced my understanding and improved the manuscript. Any errors remaining are mine. This research was supported by the Advanced Research Projects Agency of the Department of Defense and was monitored by the Air Force Office of Scientific Research under grant AFOSR-83-0037.

REFERENCES

Aki, K., Scattering and attenuation of shear waves in the lithosphere, *J. Geophys. Res.*, *85*, 6496–6504, 1980.
Aki, K., and B. Chouet, Origin of coda waves: Source, attenuation, and scattering effects, *J. Geophys. Res.*, *80*, 3322–3341, 1975.
Aki, K., and P. G. Richards, *Quantitative Seismology*, vol. II, pp. 737–744, W. H. Freeman, San Francisco, Calif., 1980.
Carmichael, R. D., and E. R. Smith, *Mathematical Tables and Formulas*, 261 pp., Dover, New York, 1962.
Chernov, L. A., *Wave Propagation in a Random Medium*, pp. 6–11 and 41–53, McGraw-Hill, New York, 1960.
Dainty, A. M., A scattering model to explain seismic Q observations in the lithosphere between 1 and 30 Hz, *Geophys. Res. Lett.*, *8*, 1126–1128, 1981.
Dainty, A. M., and M. N. Toksoz, Seismic codas on the earth and moon: A comparison, *Phys. Earth Planet. Inter.*, *26*, 250–260, 1981.
Haddon, R. A. W., and J. R. Cleary, Evidence for scattering of seismic PKP waves near the mantle-core boundary, *Phys. Earth Planet. Inter.*, *8*, 211–234, 1974.

Kikuchi, M., Dispersion and attenuation of elastic waves due to multiple scattering from inclusions, *Phys. Earth Planet. Inter.*, *25*, 159–162, 1981.

Knopoff, L., and J. A. Hudson, Frequency dependence of amplitudes of scattered elastic waves, *J. Acoust. Soc. Am.*, *42*, 18–20, 1967.

Pekeris, C. L., Comments on T. E. W. Schumann's paper "An investigation concerning G. I. Taylor's correlation coefficient of turbulence," *Philos. Mag.*, *33*, 541–543, 1942.

Pekeris, C. L., Note on the scattering of radiation in an inhomogeneous medium, *Phys. Rev.*, *71*, 268–269, 1947.

Sato, H., Amplitude attenuation of impulsive waves in random media based on travel time corrected mean wave formalism, *J. Acoust. Soc. Am.*, *71*, 559–564, 1982*a*.

Sato, H., Attenuation of *S* waves in the lithosphere due to scattering by its random velocity structure, *J. Geophys. Res.*, *87*, 7779–7785, 1982*b*.

Taylor, G. I., Diffusion by continuous movements, *Proc. London Math. Soc.*, *20*, 196–212, 1920.

Warren, N., *Q* and structure, *Moon Planets*, *4*, 430–441, 1972.

Wu, R.-S., Attenuation of short period seismic waves due to scattering, *Geophys. Res. Lett.*, *9*, 9–12, 1982.

A. M. Dainty, School of Geophysical Sciences, Georgia Institute of Technology, Atlanta, GA 30332.

(Received August 3, 1983;
revised January 9, 1984;
accepted January 17, 1984.)